THE UNIVERSITY of TENNESSEE at CHATTANOOGA

SIMCENTER

NATIONAL CENTER for COMPUTATIONAL ENGINEERING

Overset and Adaptive Meshes for Stabilized Finite-Element Scheme

W. Kyle Anderson, Behzad Ahrabi, and Chao Liu

2014 CFD Summer School

Modern Techniques for Aerodynamic Analysis and Design

Beijing Computational Sciences Research Center

July 7-11, 2014

Source of Material

- Liu, C., Newman, J., and Anderson, K., “A Streamline/Upwind Petrov-Galerkin Overset Grid Scheme for the Navier-Stokes Equations with Moving Domains,” AIAA-2014-2980, paper presented at 32nd AIAA Applied Aerodynamic Conference, Atlanta, GA, June 16-20, 2014.

- Ahrabi, B.R., Anderson, W.K., and Newman, J., “High-Order Finite-Element Method and Dynamic Adaptation for Two-Dimensional Laminar and Turbulent Navier-Stokes,” AIAA-2014-2983, paper presented at 32nd AIAA Applied Aerodynamic Conference, Atlanta, GA, June 16-20, 2014.

Overset Grid Motivation

- Advantages of finite elements
  - Extendable to high-order accuracy
  - Stencil is contained inside the element
- Benefits for overset grid schemes
  - Minimal grid overlapping required
  - Facilitates hole cutting
  - Curved geometry poses minimal difficulties

Outline

- Governing equations
- Overset methodology
- Hole cutting
- Results
  - Manufactured solutions
  - Steady turbulent flow
  - Unsteady moving boundary
  - Relative motion between two bodies
- Conclusion

Governing Equations

- Weighted intergral form of compressible Navier-Stokes equations with Spalart-Allmaras turbulence model

$$\int_{\Omega} \varphi \left[\frac{\partial Q}{\partial t} + \nabla \cdot \left(\overline{\mathbf{F}}_e(Q) - \mathbf{F}_v(Q, \nabla Q) \right) - S(Q, \nabla Q) \right] d\Omega = 0$$

- Convective flux on dynamic grids

$$\overline{\mathbf{F}}_e = \mathbf{F}_e - \mathbf{V}_g Q$$

- SUPG used in defining weighting function

$$\varphi = [N] + [P]$$

- Utilizing integration by parts the weak form becomes

$$\frac{\partial}{\partial t} \int_{\Omega} N\, \mathbf{Q}\, d\Omega - \int_{\Omega} \nabla N \cdot \left(\overline{\mathbf{F}}_e - \mathbf{F}_v \right) d\Omega + \underline{\oint_{\Gamma} N \left(\overline{\mathbf{F}}_e - \mathbf{F}_v \right) \cdot \mathbf{n}\, d\Gamma}$$

Boundary terms

$$- \int_{\Omega} N\, S\, d\Omega + \frac{\partial}{\partial t} \int_{\Omega} [P] \mathbf{Q}\, d\Omega + \int_{\Omega} [P] \left(\nabla \cdot \left(\overline{\mathbf{F}}_e - \mathbf{F}_v \right) - S \right) d\Omega = 0$$

Outline

- Governing equations
- Overset methodology
- Hole cutting
- Results
  - Manufactured solutions
  - Steady turbulent
  - Unsteady moving boundary
  - Relative motion between two bodies
- Conclusion

Overset Methodology

- Overset problems appear as boundary conditions

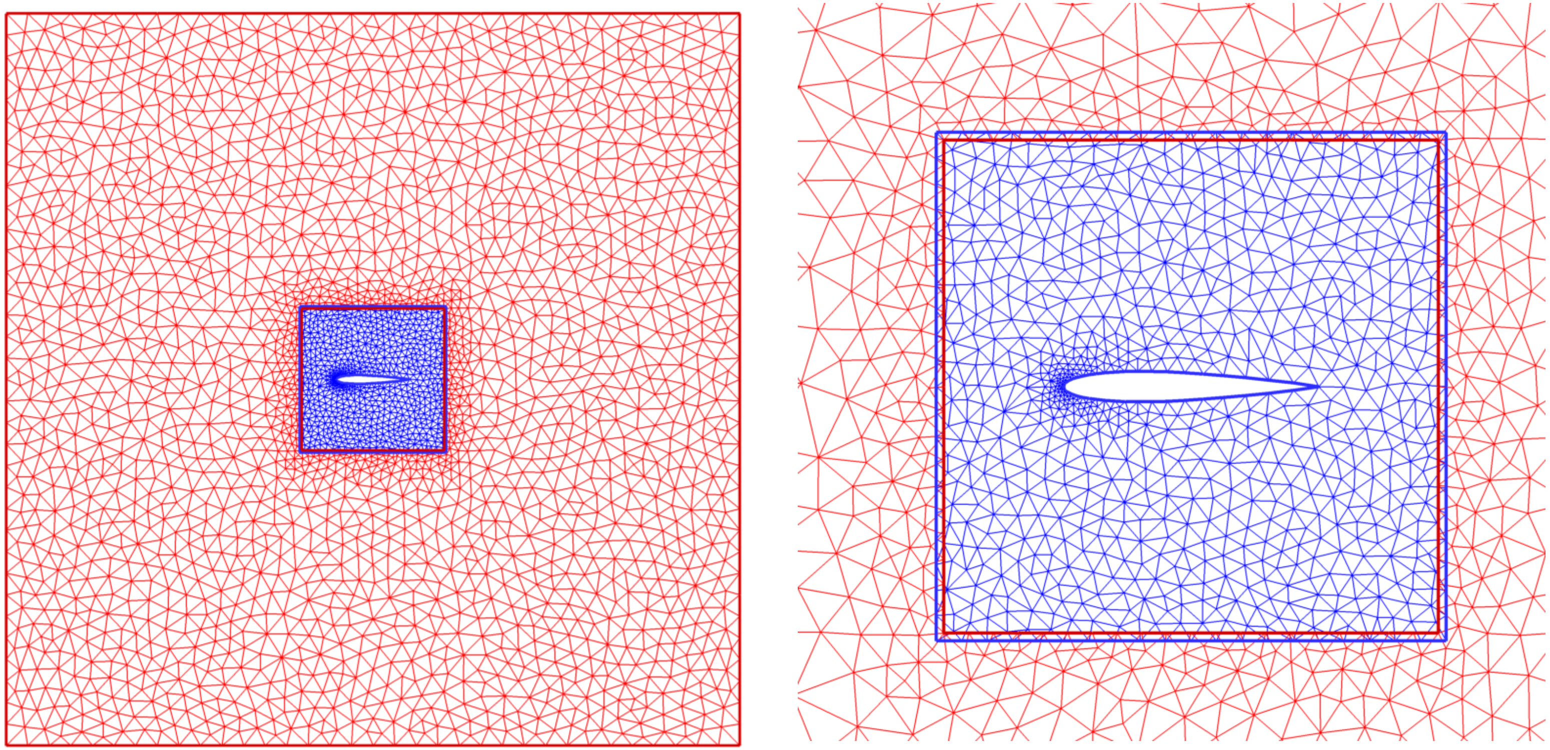

Example of overset problem of an airfoil

Discretization

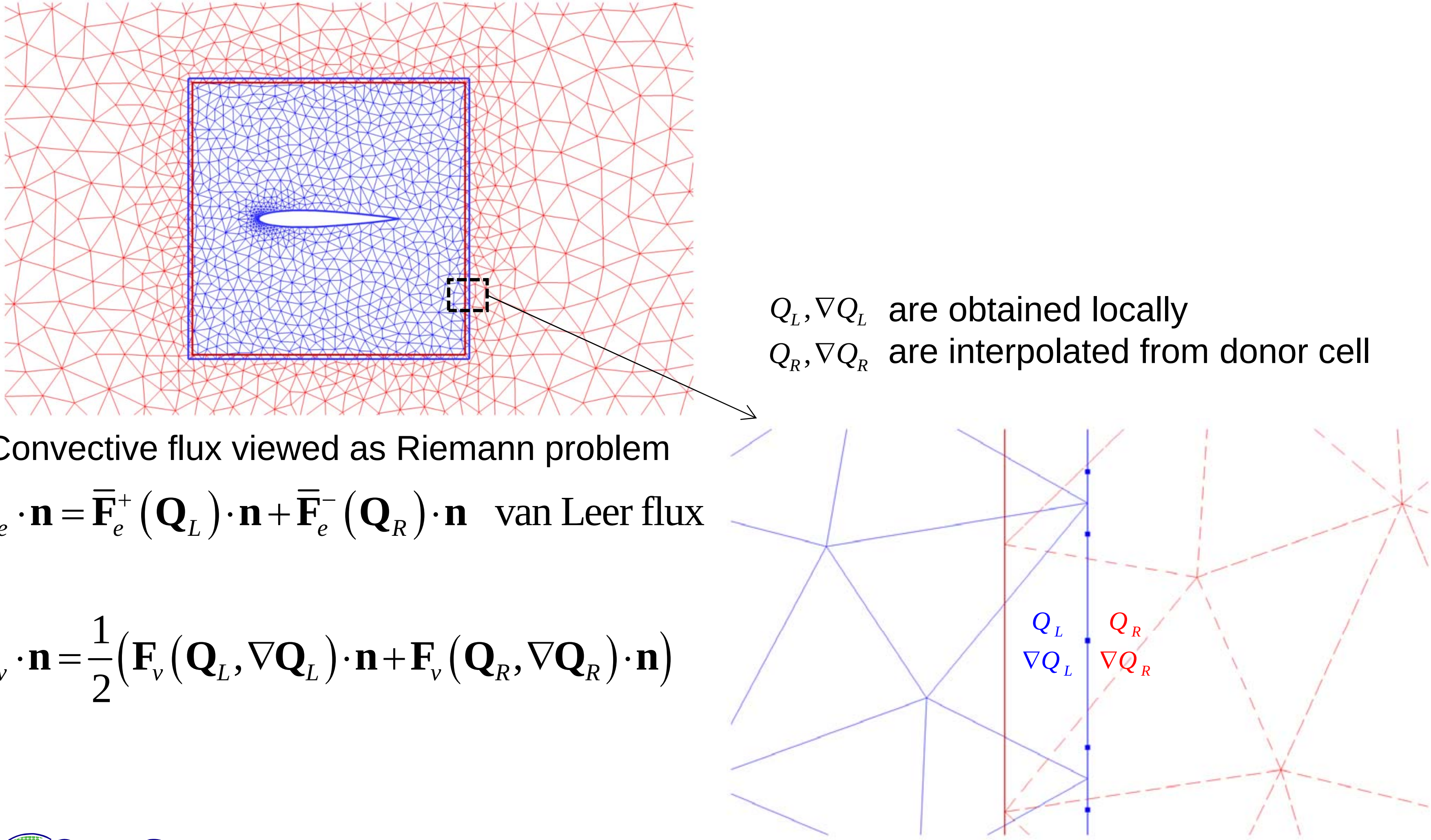

$Q_L, \nabla Q_L$ are obtained locally

$Q_R, \nabla Q_R$ are interpolated from donor cell

Convective flux viewed as Riemann problem

$$\overline{\mathbf{F}}_e \cdot \mathbf{n} = \overline{\mathbf{F}}_e^+ \left(\mathbf{Q}_L\right) \cdot \mathbf{n} + \overline{\mathbf{F}}_e^- \left(\mathbf{Q}_R\right) \cdot \mathbf{n} \quad \text{van Leer flux}$$

$$\mathbf{F}_v \cdot \mathbf{n} = \frac{1}{2}\left(\mathbf{F}_v\left(\mathbf{Q}_L, \nabla \mathbf{Q}_L\right) \cdot \mathbf{n} + \mathbf{F}_v\left(\mathbf{Q}_R, \nabla \mathbf{Q}_R\right) \cdot \mathbf{n}\right)$$

Outline

- Governing equations
- Overset methodology
- Hole cutting
- Results
  - Manufactured solutions
  - Steady turbulent
  - Unsteady moving boundary
  - Relative motion between two bodies
- Conclusion

Hole Cutting

- Hole cutting includes two steps
  - Identify invalid cells
  - Selection among valid cells

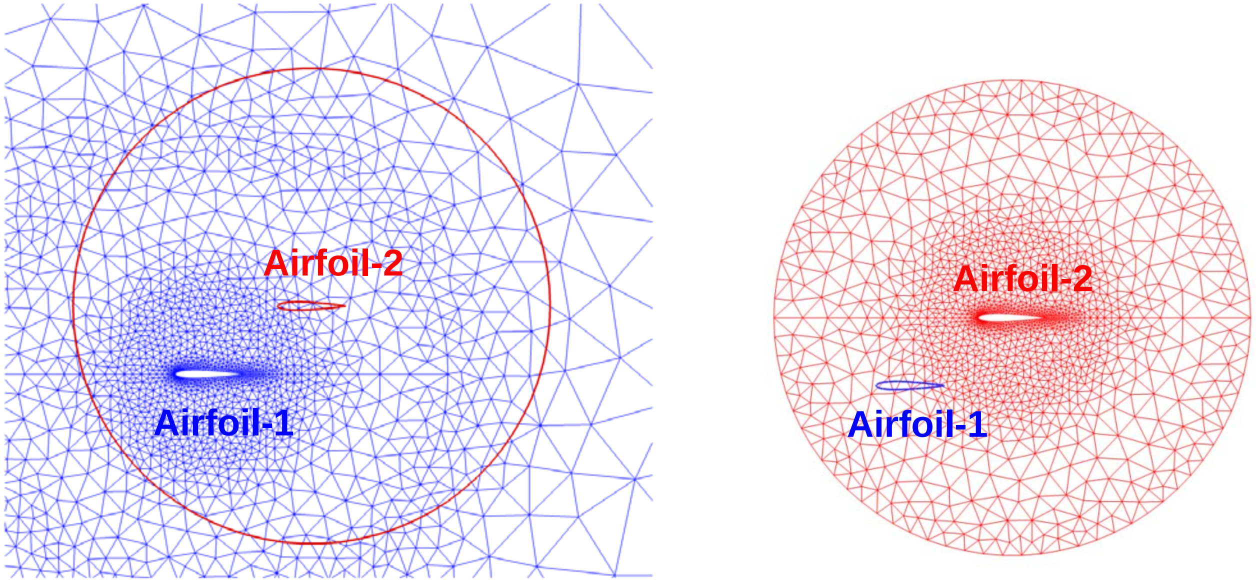

Grid-1

Grid-2

Example of 2 airfoil overset grids

Identify Invalid Cells

- On Grid-1, determine location of Airfoil-2. Cells in Grid-1 that intrude or lie inside of Airfoil-2 are invalid, and need to be removed from domain. Repeat procedure on Grid-2 for Airfoil-1.
- Direct wall cut is used to identify invalid cells

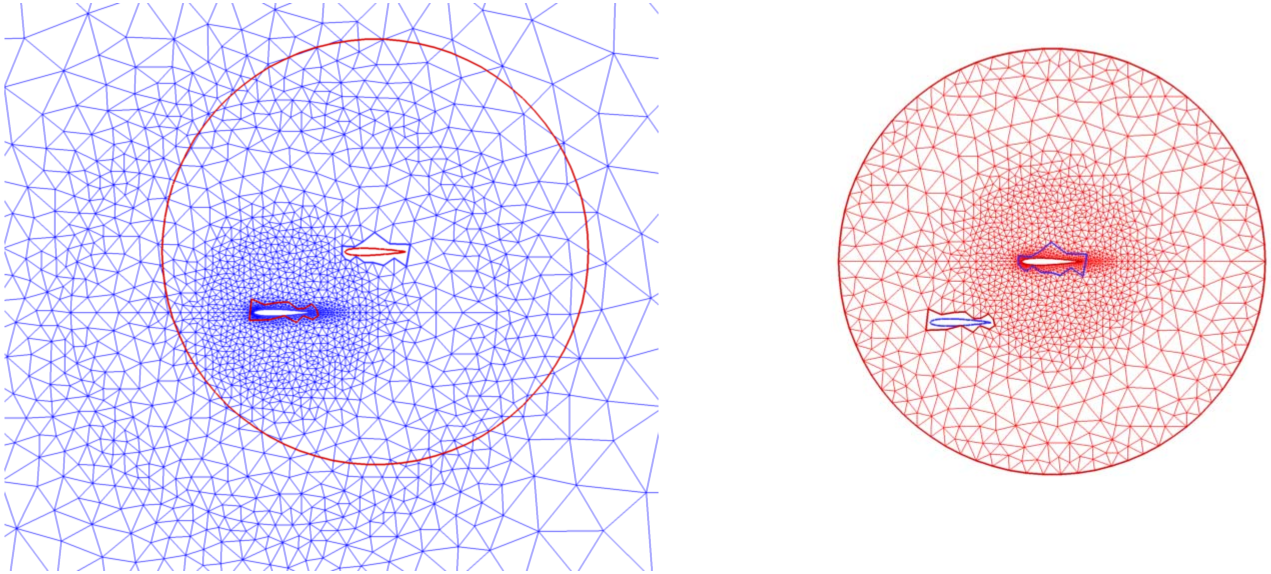

Grid 1

Grid 2

Grids after direct wall cut (all invalid cells removed)

Select Among Valid Cells

- To minimize grid overlapping, among the valid cells, certain cells are selected for simulation, the remainder are removed.
- No definitive selection process. Three approaches are explored:
  - Existing Implicit Hole Cutting (IHC) method
  - Proposed modified Implicit Hole Cutting method
  - Novel Elliptic Hole Cutting (EHC) method

Original IHC

- Developed by Lee & Baeder, 2008
- A cell select process based on *cell-quality*
  - Each grid node is viewed as a sampling point
  - For each sampling point, all cells that contain it are identified
  - Among the list of cells, the one with highest *cell-quality* is kept, then remainders are removed
- *cell-quality* is a user-defined grid metric (inverse of cell volume, aspect ratio, and so on...)
- User can manually specify cell-quality of some cells to influence selection process
- User does not have to specify grid priority
- However, if no grid priority is specified, selected cells may NOT be distributed "continuously"

Original IHC

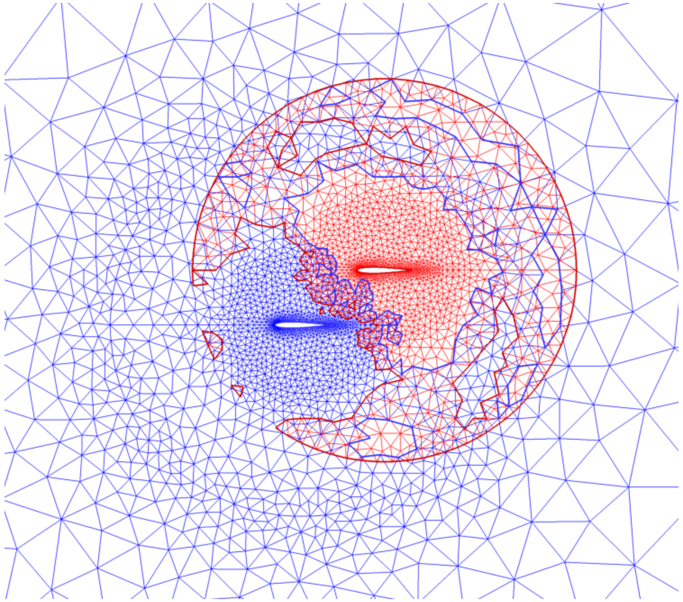

Mesh after original IHC

- *Cell-quality* defined as the inverse of cell volume
- Smallest cells are selected across the whole domain
- High *cell-quality* does not gurantee a high-quality overset mesh. "Continuity" of cell selection is often more important

Modified IHC

- Introduce grid *priority-factor* in favor of mesh "continuity"

$$priority\_factor(iGrid) = 1 + C\frac{n(iGrid) - n_{\min}}{n_{\max} - n_{\min}}$$

- Use original IHC to provide an initial cell selection
- In one cell selection iteration
  - Loop over each sampling point
    - Recalculate grid *priority-factor* for each grid at that sampling point. Higher *priority-factor* is given to the grid that is selected by more neighboring sampling points
    - The cell with the highest *priority-factor*cell-quality* is selected at that sampling point
- The process iterates until the cell selection stops changing

Modified IHC

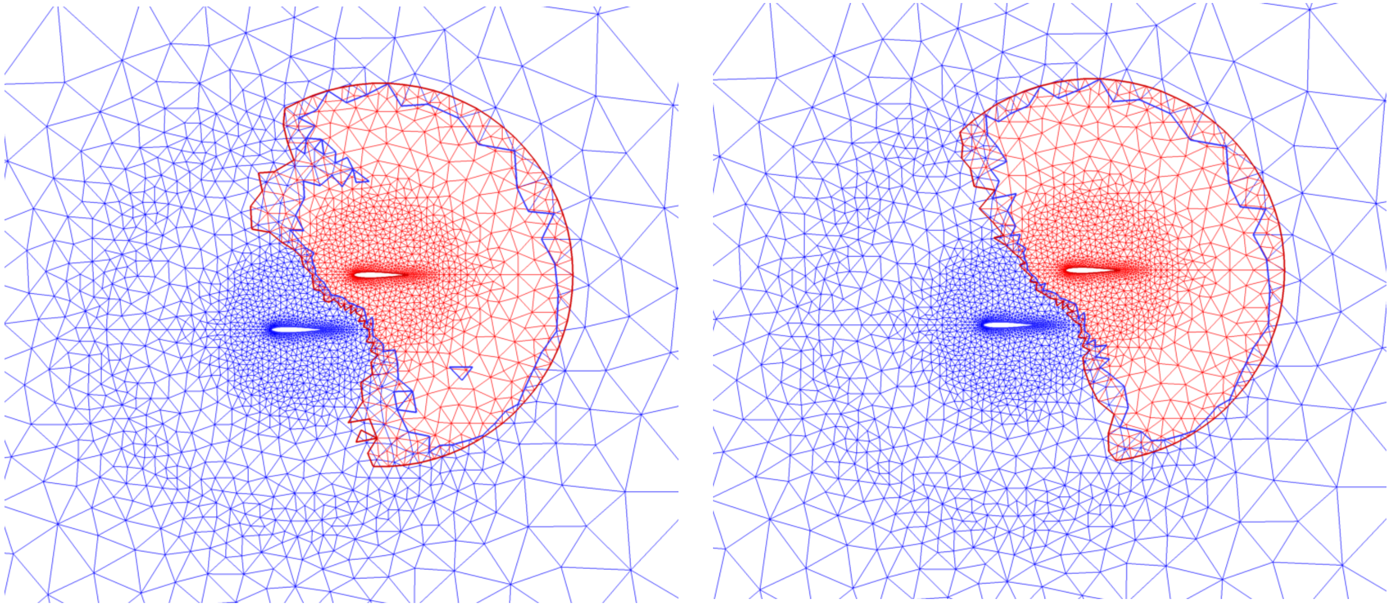

After 1 cell-selection iteration

After 5 cell-selection iteration

Cell selection using modified IHC (original IHC is used to provide the initial selection)

Elliptic Hole Cutting

- New approach. Details in final updated paper
- Solve a Poisson equation on each grid. Select the cells with the highest pseudo temperature.

$$\nabla^2 T = f$$

- Boundary conditions
  - Invalid nodes are set to minimum value (T= -1)
  - Nodes that must be selected (i.e. nodes in non-overlap regions) are set to maximum value (T= 1)
  - Overset boundaries (before hole cutting) are treated as adiabatic wall (T_n= 0)
- No need to solve the exact Poisson problems
- No need for the solutions to fully converge

Elliptic Hole Cutting

- Choices of source term
  - In favor of *cell-quality*

$$f = f_{\text{global\_min}} + \frac{c - c_{\text{local\_min}}}{c_{\text{local\_max}} - c_{\text{local\_min}}} \left(f_{\text{global\_max}} - f_{\text{global\_min}} \right)$$

where *c* is *cell-quality*

  - In favor of specific grids

$$f = \begin{cases} f_{\max} & \text{for prefered grids} \\ f_{\min} & \text{for other grids} \end{cases}$$

  - Other choices of source term possible

Elliptic Hole Cutting

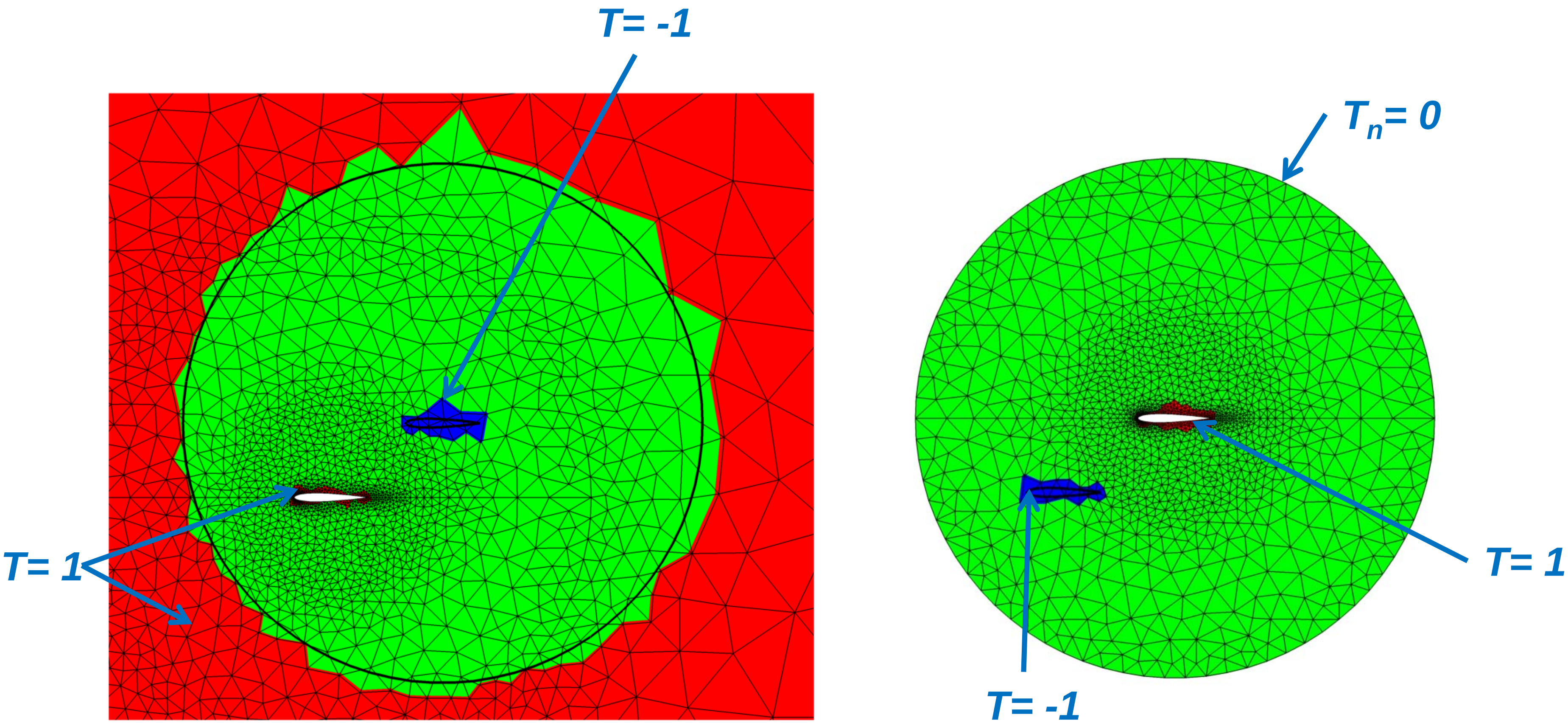

Grid 1

Grid2

Boundary conditions for Poisson equations on each grid

Elliptic Hole Cutting

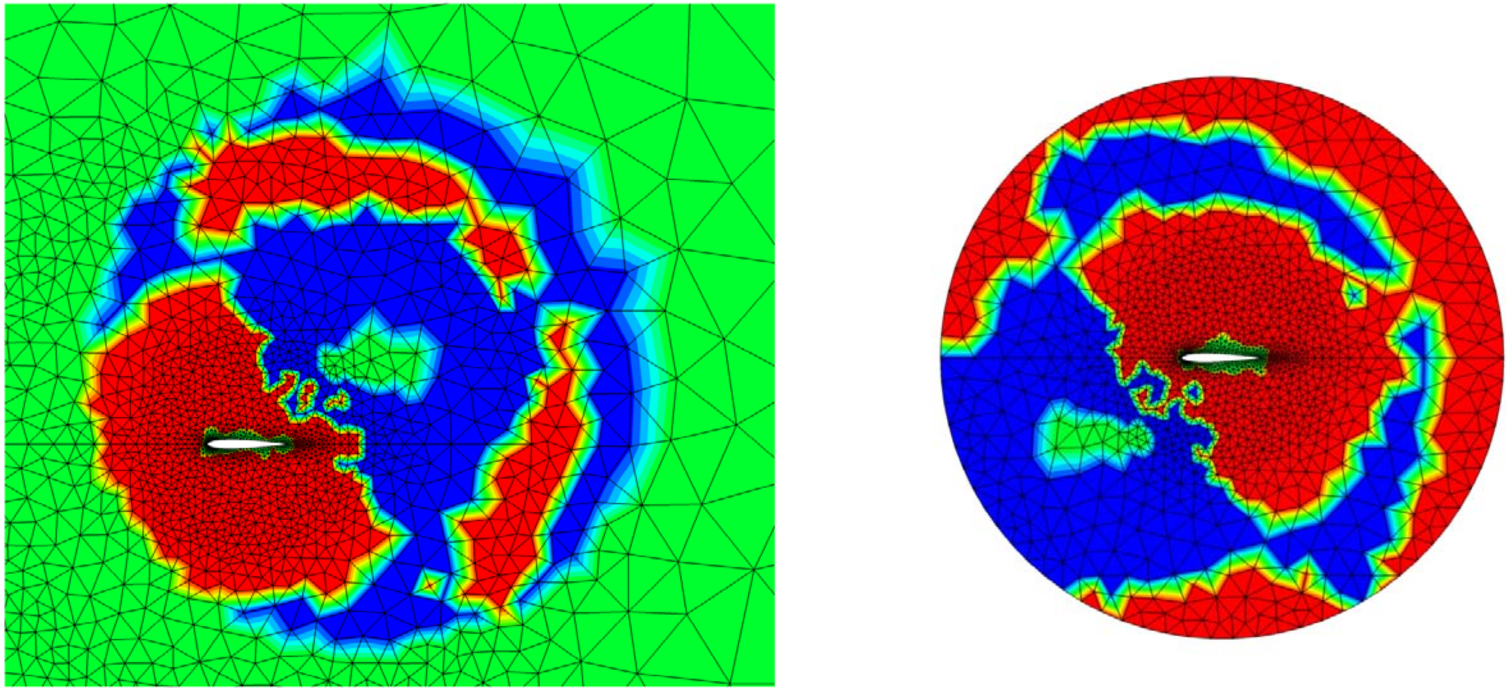

Grid 1

Grid2

Source term for the Poisson problems in favor of cell-quality

Elliptic Hole Cutting

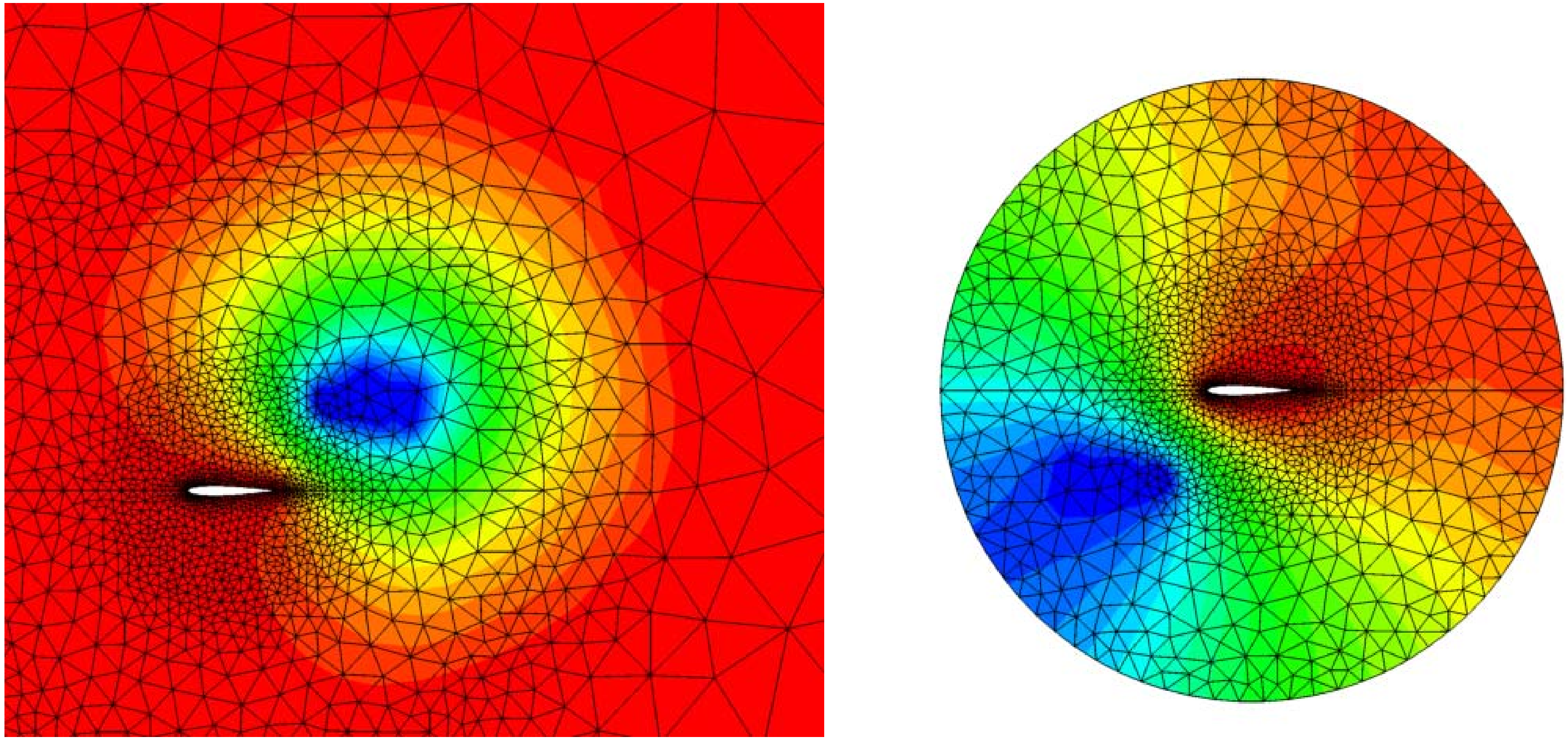

Grid 1

Grid 2

Solution of Poisson problems

Elliptic Hole Cutting

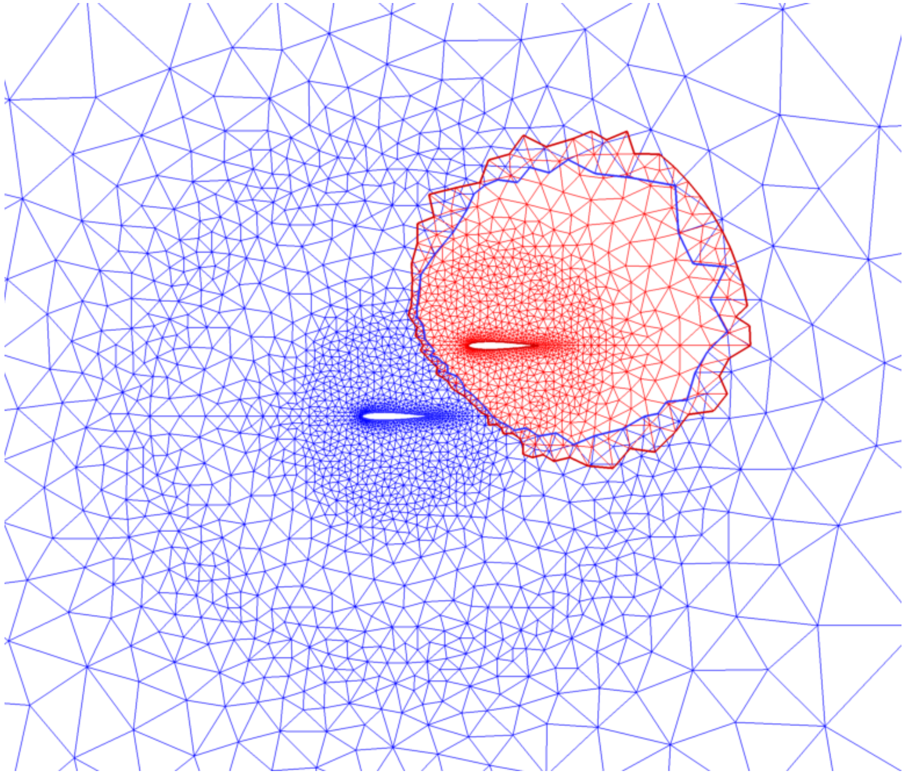

Final mesh

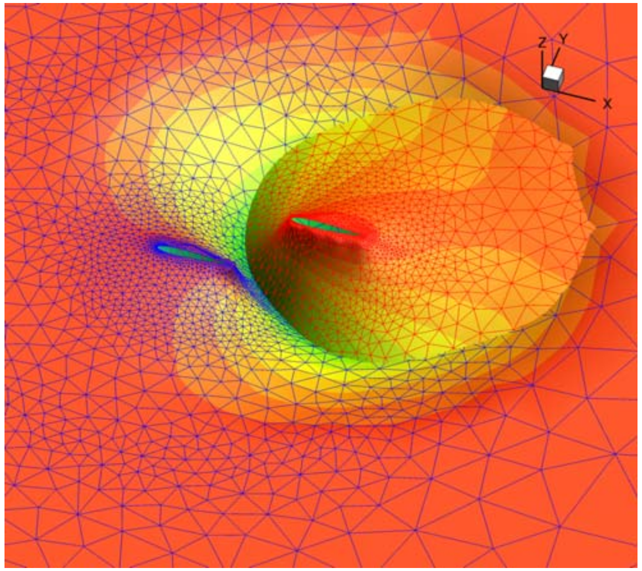

3D view of Poisson solution

Comparison of Hole Cutting

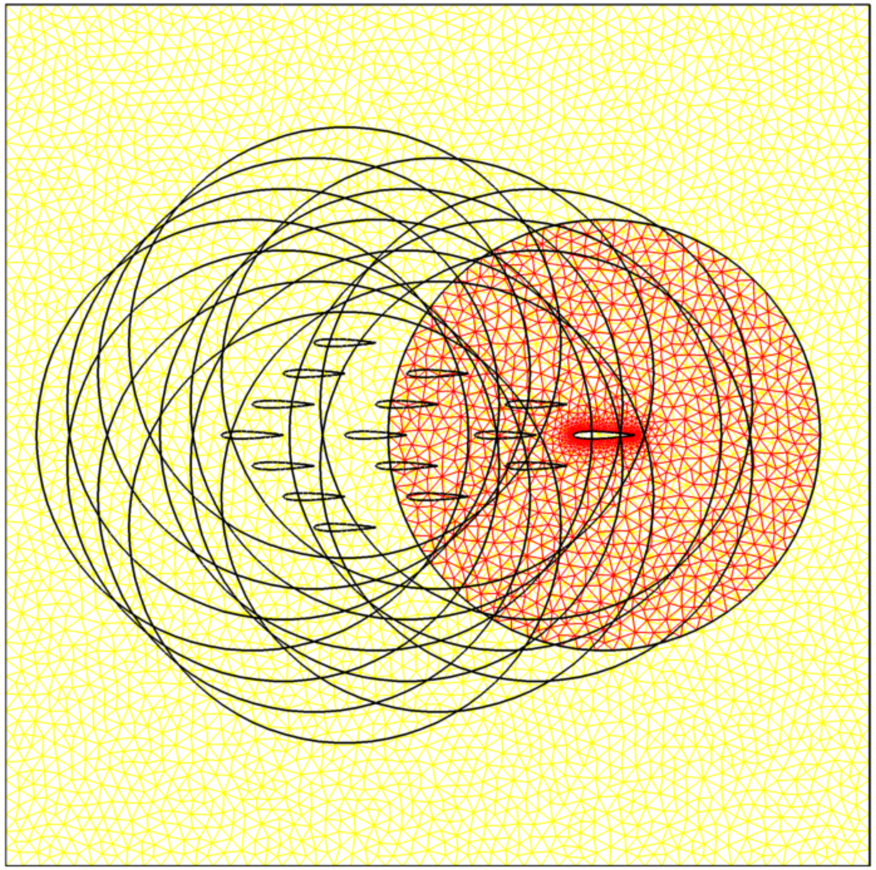

16 airfoil-grids overlapping on a background grid

Comparison of Hole Cutting

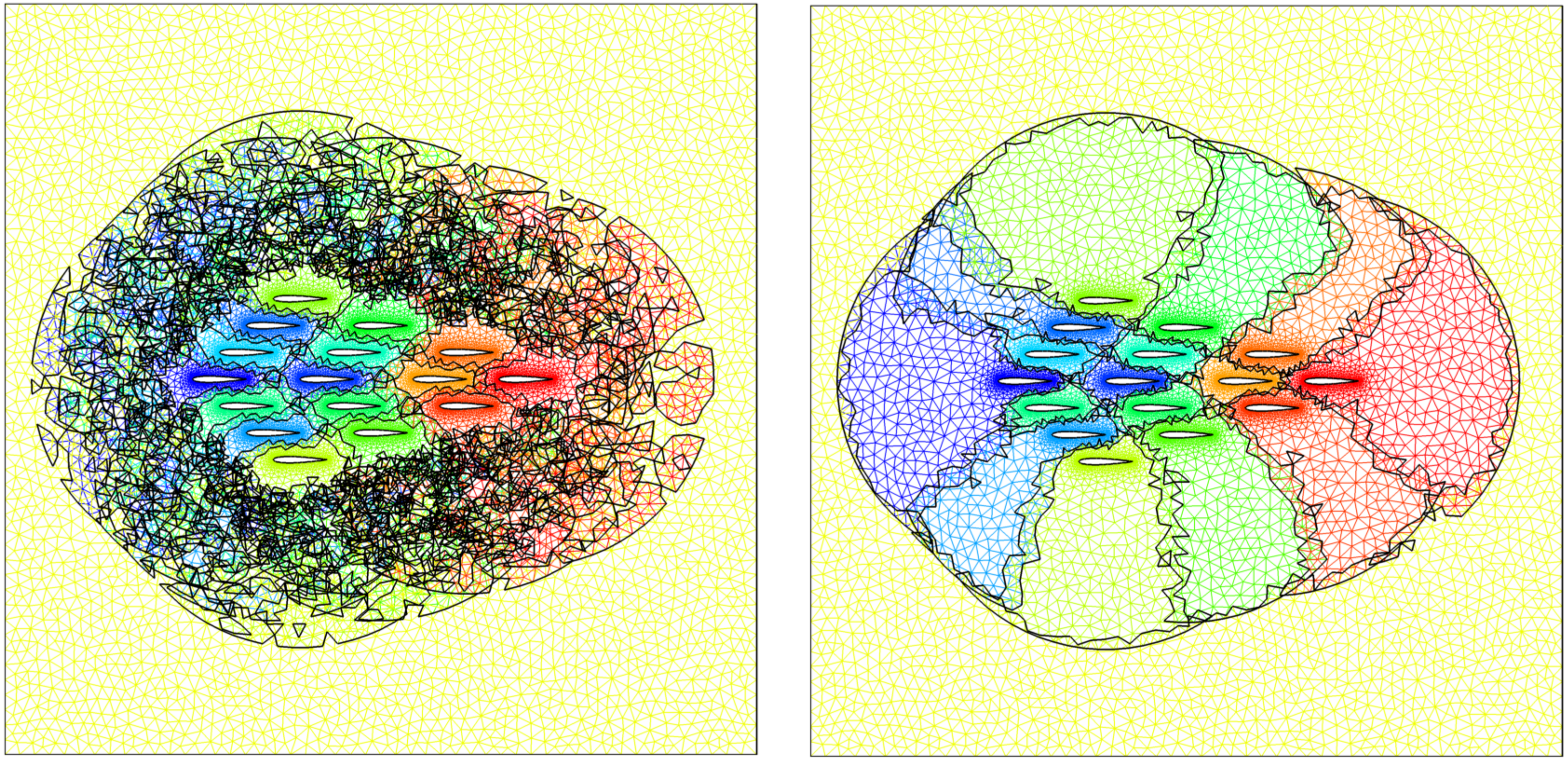

Original IHC

Modified IHC

Original and modified Implicit Hole Cutting

Comparison of Hole Cutting

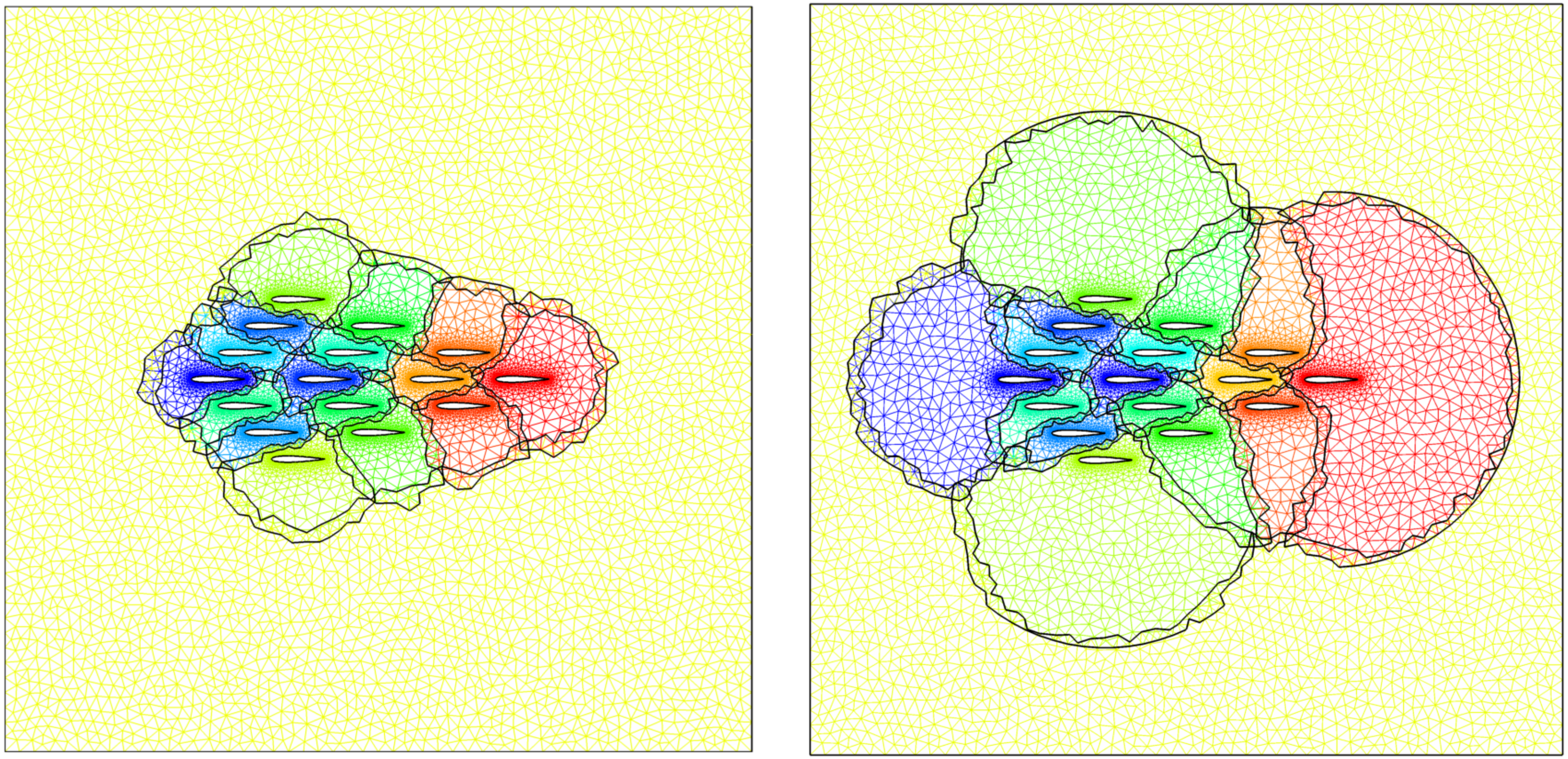

In favor of cell quality

In favor of airfoil grids

Elliptic Hole Cutting using different source terms

Advantages of Elliptic Hole Cutting

- Automation, does not require user input, yet the "continuity" of cell selection is still guaranteed by the smoothness of the Poisson solutions
- Users still have the freedom to influence cell selection process (in favor of cell quality, specific grids, etc…) by devising different source terms, or even different boundary conditions

Outline

- Governing equations
- Overset methodology
- Hole cutting
- Results
  - Manufactured solutions
  - Steady turbulent
  - Unsteady moving boundary
  - Relative motion between two bodies
- Conclusion

Manufactured Solutions

- The Method of Manufactured Solution (MMS) is a general procedure for generating nontrivial exact solutions to PDEs
- Accuracy of the SUPG overset scheme is assessed using MMS based on a comprehensive set of guidelines

Manufactured Solutions

- MMS for both inviscid and laminar (Re=100) equations are performed to assess accuracy
- The following trigonometric functions are used to derive forcing functions and boundary conditions

$$\rho = \rho_o\{1 + 0.2\cos[\pi(c_1x - s_1y)] + 0.2\cos[\pi(c_1x + s_1y)]\}$$
$$u = u_o\{1 + 0.2\cos[\pi(c_2x - s_2y + 0.1)] + 0.2\cos[\pi(c_2x + s_2y + 0.1)]\}$$
$$v = v_o\{1 + 0.2\cos[\pi(c_3x - s_3y - 0.1)] + 0.2\cos[\pi(c_3x + s_3y + 0.1)]\}$$
$$T = T_o\{1 + 0.2\cos[\pi(c_4x - s_4y - 0.1)] + 0.2\cos[\pi(c_4x + s_4y - 0.1)]\}$$

  - ρ_o, u_o, v_o, T_o correspond to the free stream condition of $M = 0.2, \alpha = 15^\circ$
  - c_i, s_i correspond to cosine and sine of 0°, 40°, 80°, and 120°

Manufactured Solutions

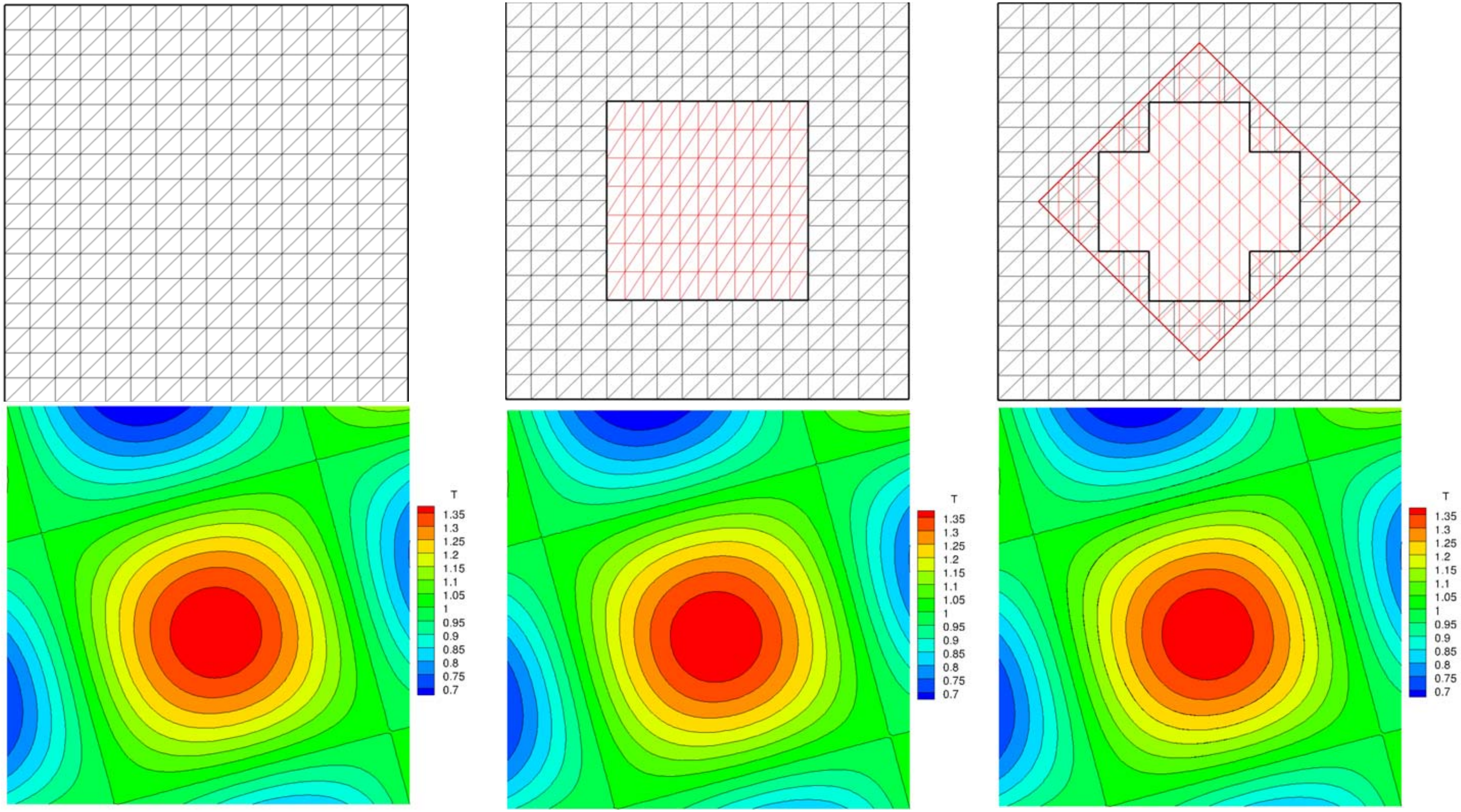

Temperature on coarsest meshes, laminar, P3 elements

Manufactured Solutions

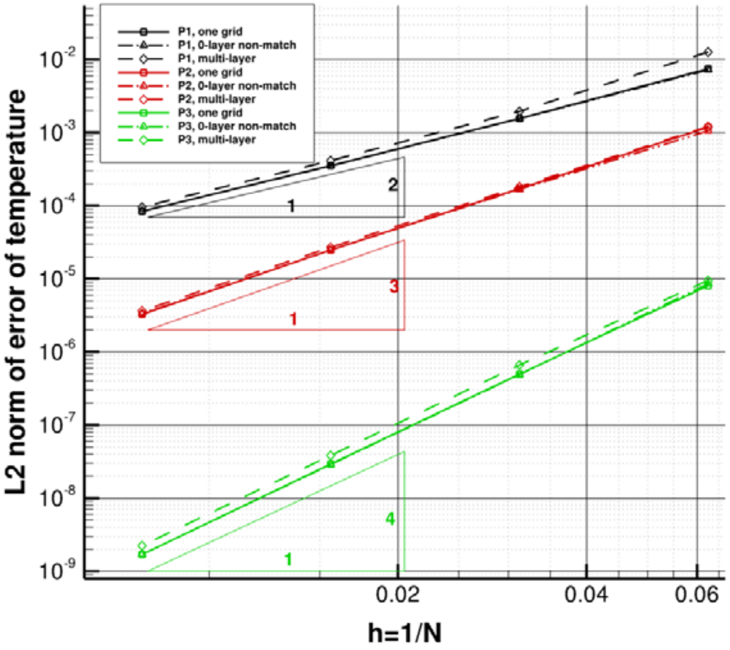

Temperature, invisicd

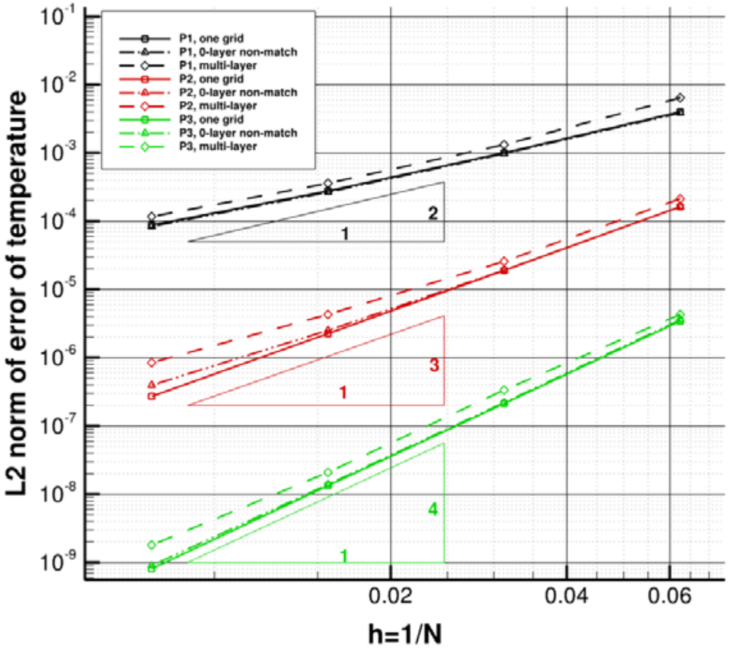

Temperature, laminar

Order of accuracy for inviscid and laminar flow

Outline

- Governing equations
- Overset methodology
- Hole cutting
- Results
  - Manufactured solutions
  - Steady turbulent
  - Unsteady moving boundary
  - Relative motion between two bodies
- Conclusion

Steady Turbulent Flow

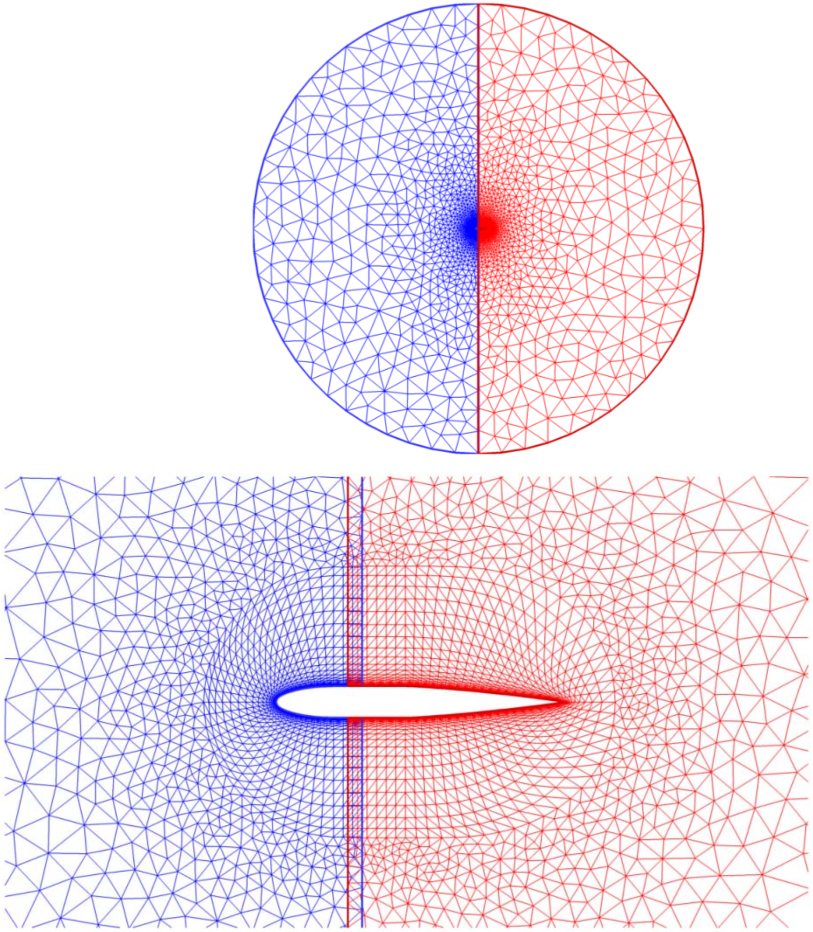

Free stream condition

$$M_{\infty} = 0.2, \alpha_{\infty} = 2^{\circ}, \mathrm{Re} = 10^{6}$$

Spalart-Allmaras turbulent model
y+ of wall spacing is 1

Steady Turbulent Flow

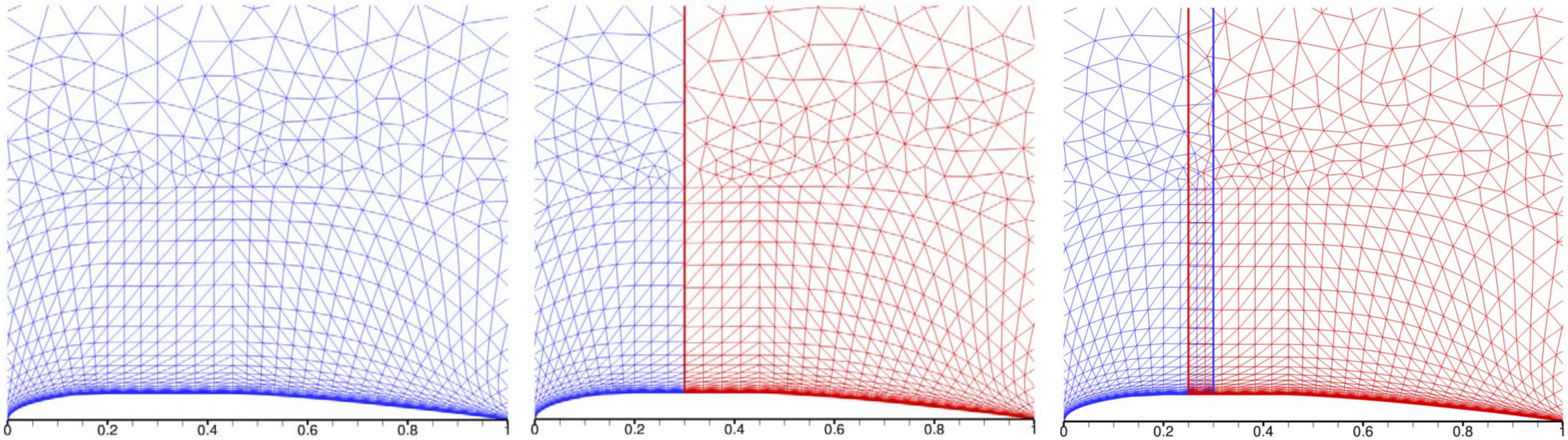

Single grid

Zero-layer non-matched overset grid

Multi-layer overlapping overset grid

Grids used in simulations

Steady Turbulent Flow

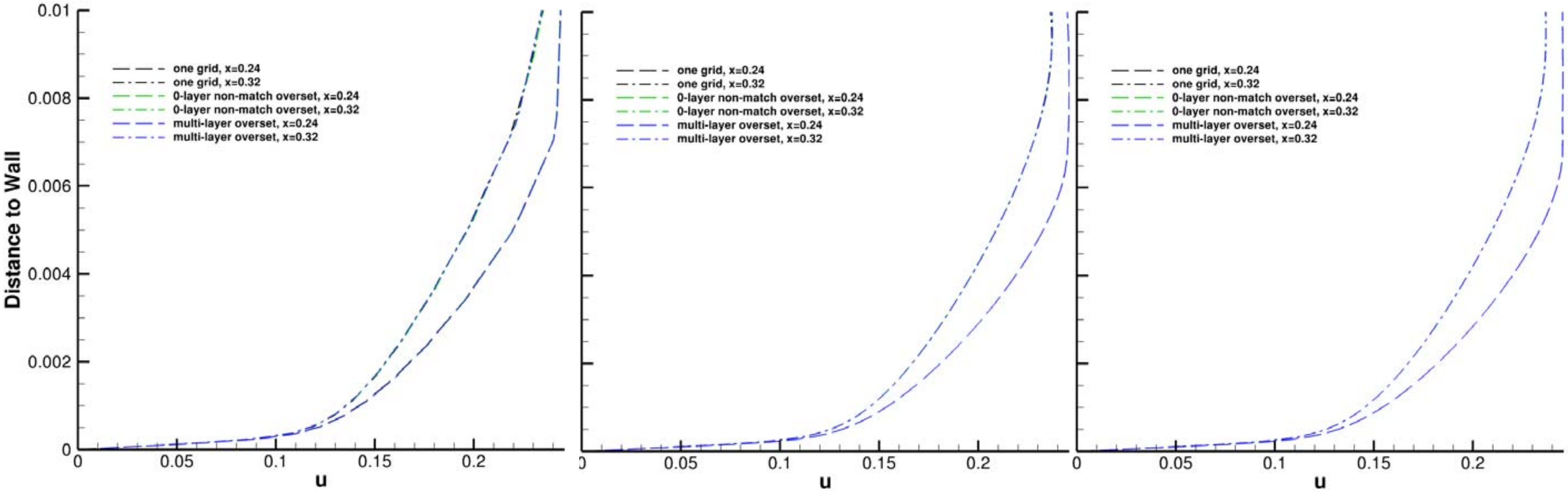

P1 elements

P2 elements

P3 elements

X-velocity profile at x=0.24 and 0.32

Outline

- Governing equations
- Overset methodology
- Hole cutting
- Results
  - Modified preconditioner
  - Manufactured solutions
  - Steady turbulent
  - Unsteady moving boundary
    - Sinusoidally oscillating airfoil
    - Sinusoidally pitching and plunging airfoil
  - Relative motion between two bodies
- Conclusion

Sinusoidally Oscillating Airfoil

- Benchmark case for dynamic mesh code validation
- Free stream $M_\infty = 0.6, \alpha_\infty = 0^\circ$
- NACA0012 airfoil pitch about its quarter chord

$$\alpha(t) = \alpha_m + \alpha_o \sin(2kM_\infty t)$$

$$\text{where } \alpha_m = 2.89^\circ, \alpha_0 = 2.41^\circ, k = 0.0808$$

Sinusoidally Oscillating Airfoil

- Inviscid. P1 elements
- Multiple layers of overlap, grids generated a priori
- Grid moves as a rigid body. Analytical grid velocities are used
- For overset simulation, background grid is stationary, only airfoil grid is moving

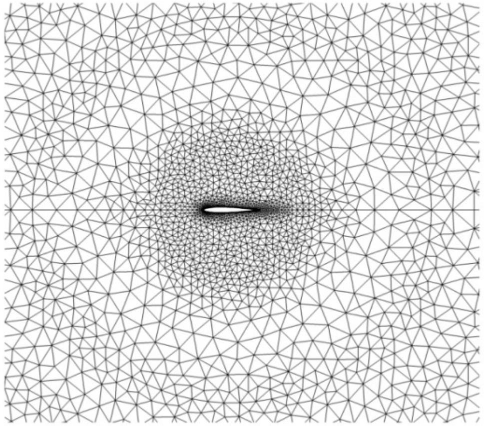

Single grid

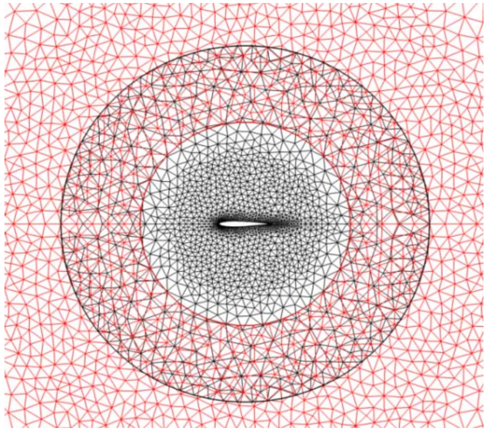

Overset grids

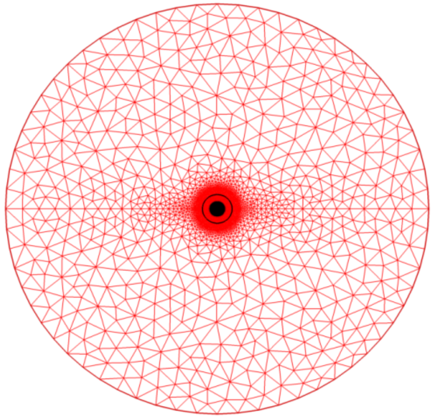

Global view of overset grids

Sinusoidally Oscillating Airfoil

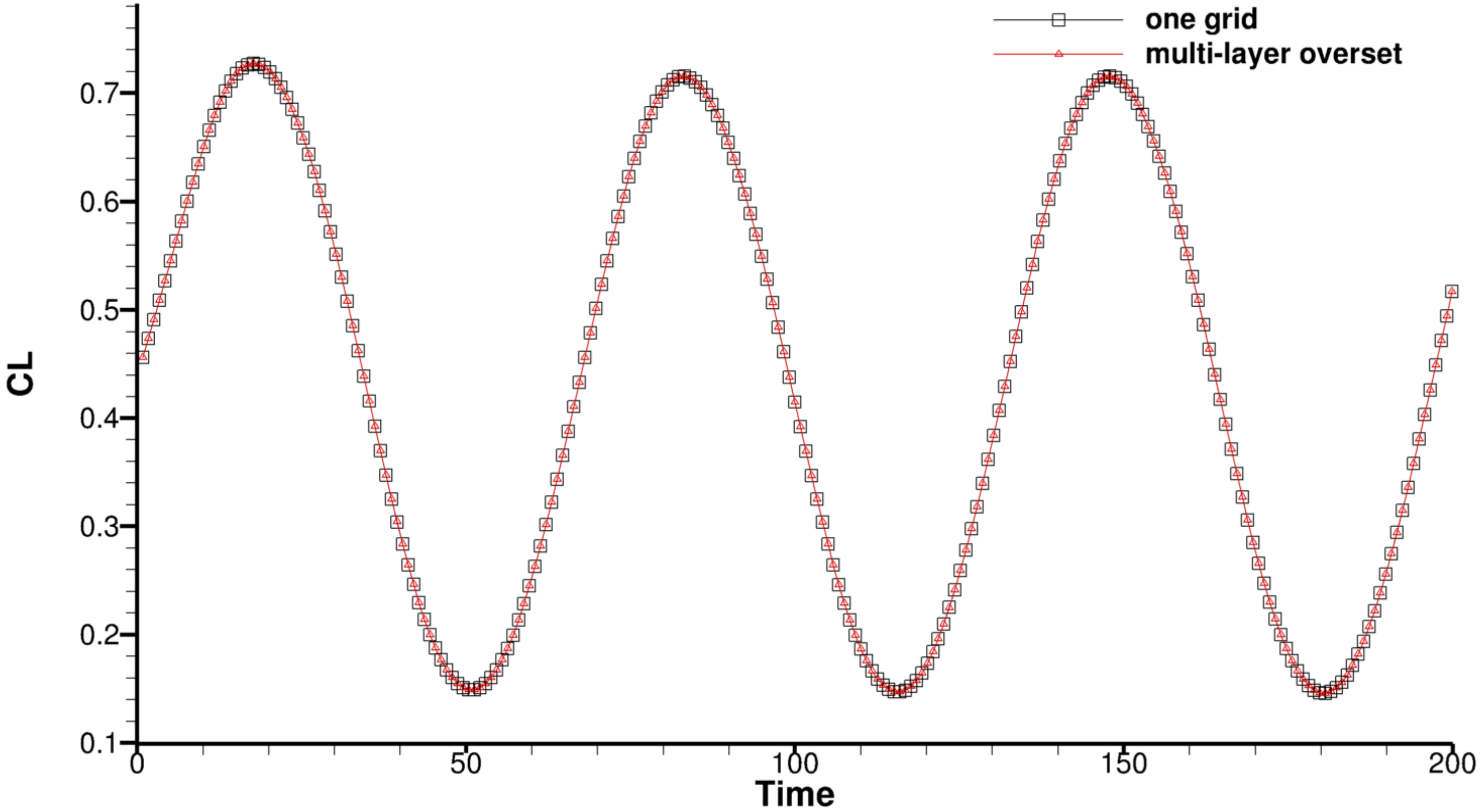

Time history of coefficient of lift

Sinusoidal Pitch and Plunge Airfoil

- Free stream $M_\infty = 0.4, \alpha_\infty = 0^\circ$
- NACA0012 Airfoil pitch about its quarter chord, and plunge

$$\begin{cases} \alpha(t) = & \alpha_m + \alpha_o \sin(2kM_\infty t) \\ h(t) = & h_0 \sin(kM_\infty t) \end{cases}$$

where $\alpha_m = 0^\circ, \alpha_0 = 5^\circ, k = 0.0808, h_0 = 0.4c,$ c is the chord length

Sinusoidal Pitch and Plunge Airfoil

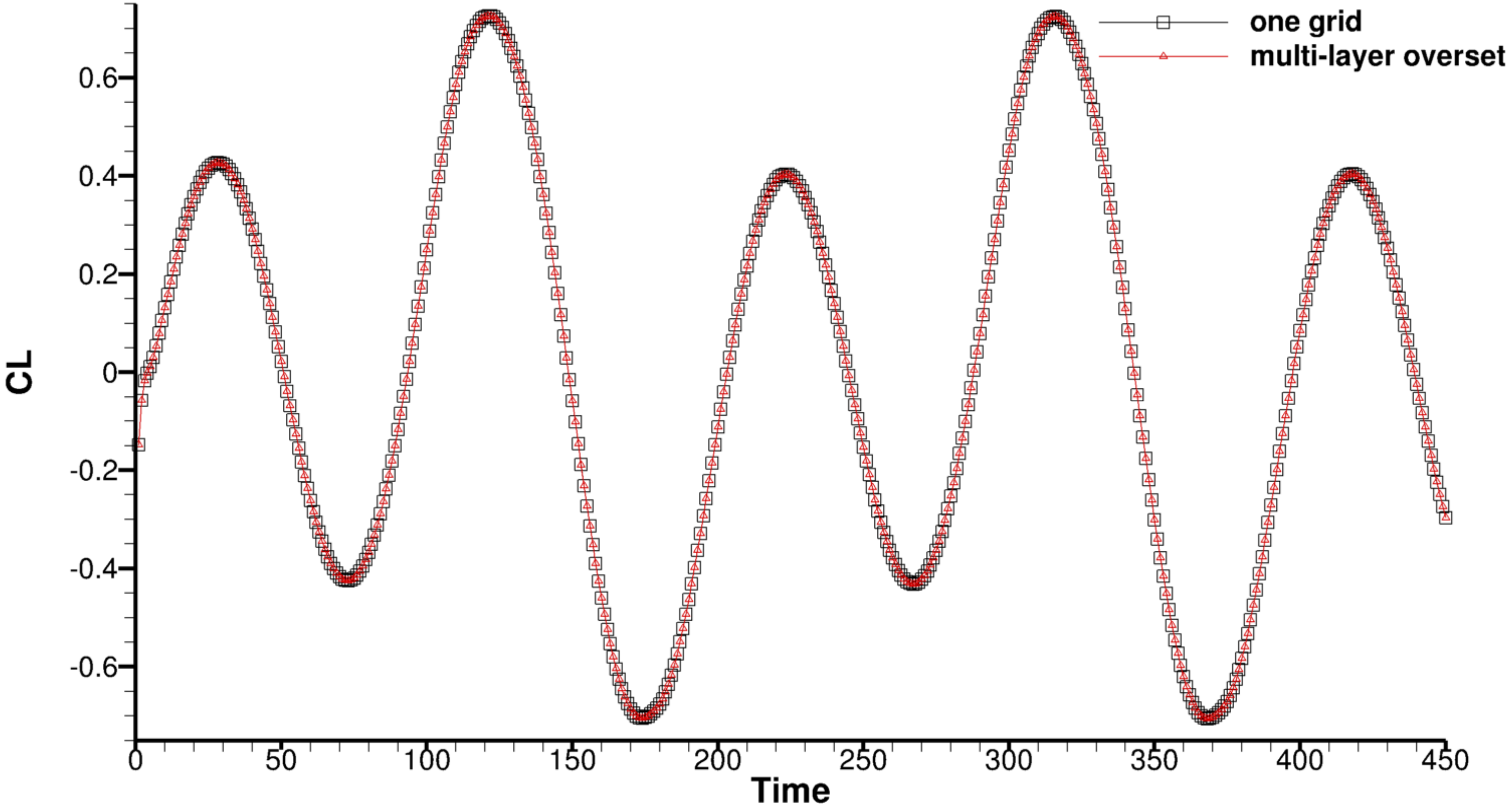

Time history of coefficient of lift

Outline

- Governing equations
- Overset methodology
- Hole cutting
- Results
  - Manufactured solutions
  - Steady turbulent
  - Unsteady moving boundary
  - Relative motion between two bodies
- Conclusion

Relative Motion Between Two Bodies

- Inviscid simulation
- Demonstration of dynamic hole cutting
- Free stream $M_\infty = 0.1, \alpha_\infty = 0^\circ$
- Airfoil is stationary. Triangle wedge moves upstream at $M = 0.1$
- Non-dimensional chord length = 1
- Non-dimensional time step = 0.05
- Modified IHC is used

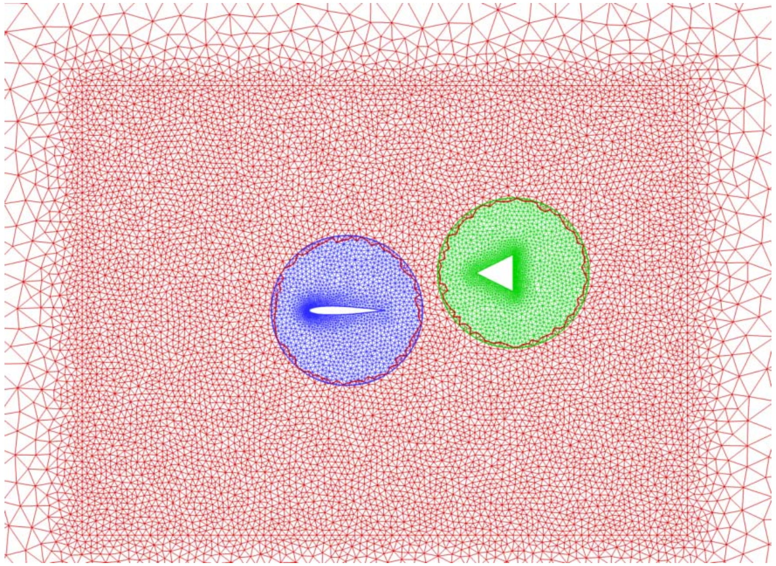

Relative Motion Between Two Bodies

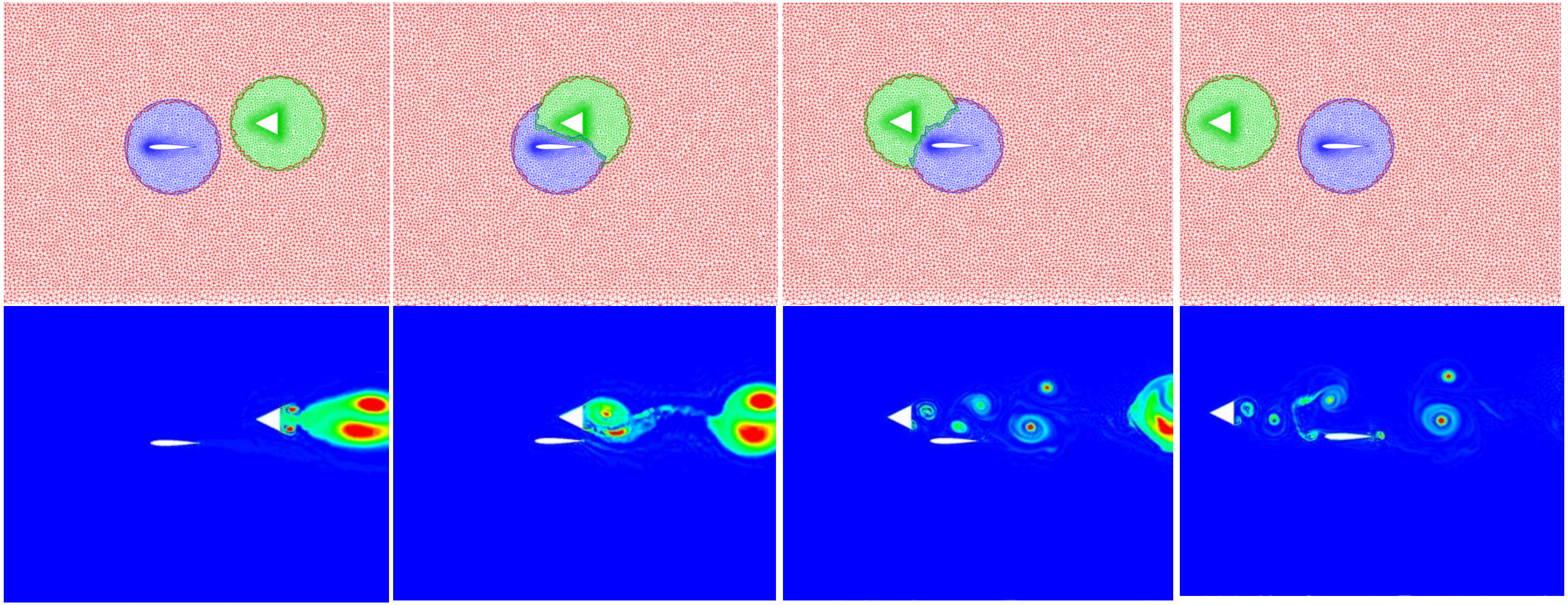

t=3 t=20 t=34 t=43

Grids (after hole cutting) and entropy contour

Outline

- Governing equations
- Overset methodology
- Hole cutting
- Results
  - Manufactured solutions
  - Steady turbulent
  - Unsteady moving boundary
  - Relative motion between two bodies
- Conclusion

Conclusion for Overset Grids

- Development of a novel hole cutting procedure: Elliptic Hole Cutting
- Demonstrated that the design order of accuracy of the method is retained using the method of manufactured solutions
- Demonstrated the method for steady-turbulent and for dynamic moving boundary simulations
- First implementation of a high-order SUPG overset grid scheme

Adaptive Meshing

- ➡ Motivation
- Mesh Modification Mechanisms
- Governing Equations and Discretization
- Adaptation Criteria
- Numerical Results
- Conclusions

Motivation

- Streamline/Upwind Petrov-Galerkin (SUPG) scheme:
  - For lower polynomial degrees, requires significantly less computational resources.
  - Great potential to be enhanced by adaptation.

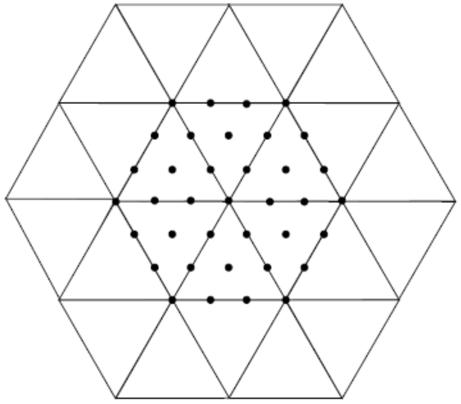

Forth order PG

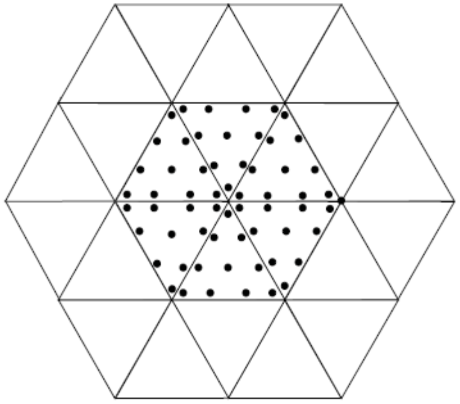

Forth order DG

Outline

- Motivation
- ➡ Mesh Modification Mechanisms
- Governing Equations and Discretization
- Adaptation Criteria
- Numerical Results
- Conclusions

Mesh Modification Mechanisms

- H-adaptation
- P-adaptation
- Hp-adaptation
  - ➢ Smoothness indicator [Persson and Peraire]

Discretization error:

$$O(h^{p+1})$$

- Non-conformal refinement
- Constraint approximation

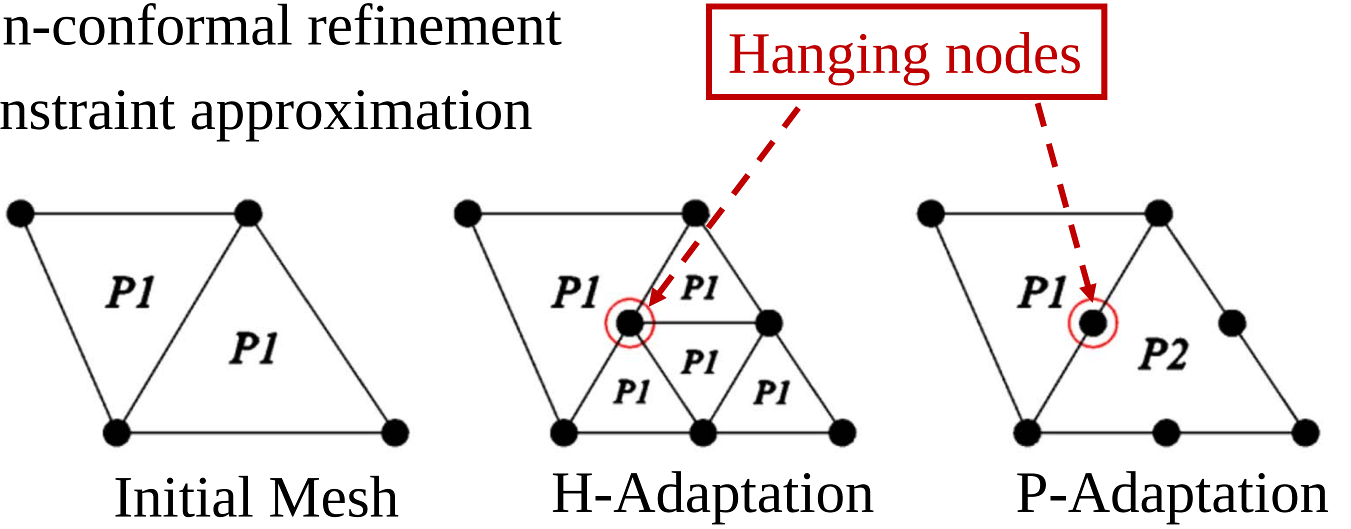
Hanging nodes

Initial Mesh H-Adaptation P-Adaptation

Outline

- Motivation
- Mesh Modification Mechanisms
- ➡ Discretization
- Adaptation Criteria
- Numerical Results
- Conclusions

Discretization

- Tessellation: $\Omega = \bigcup_e \Omega^e$
- Nodal-piecewise construction: $\hat{\mathbf{U}} = \sum_{i=1}^{nn} \mathbf{U}_i N_i$

$$\{e_i\} = \{e0, e1, e2, e3, e4, e5\}$$

$$N_i = \bigcup_{e \in \{e_i\}} N_{j_i}^e$$

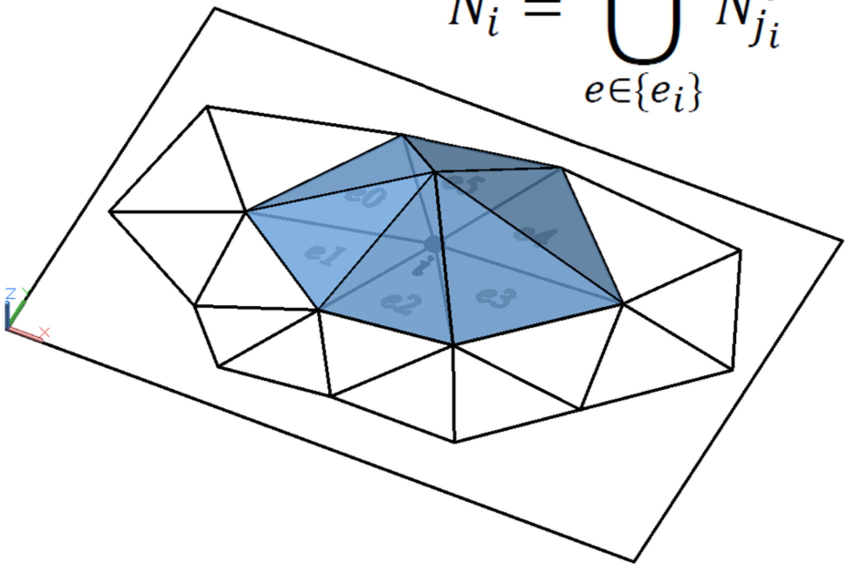

Top view

Iso-view

Discretization

- Weighted residual form: $$\int_{\Omega} \phi \left[\frac{\partial \widehat{\mathbf{U}}}{\partial t} + \nabla \cdot \mathbf{F} - \mathbf{S} \right] d\Omega = 0$$

Weight Function

- For SUPG scheme: $$\phi_i = N_i + P_i$$

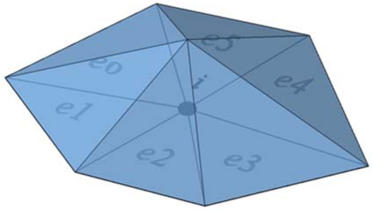

Galerkin Part

Stabilization Part

$$\int_{\Omega^e} N_i \left[\frac{\partial \widehat{\mathbf{U}}}{\partial t} - \mathbf{S} \right] d\Omega^{\mathrm{e}} + \boxed{\int_{\Omega^e} N_i \, [\nabla \cdot \mathbf{F}] d\Omega^{\mathrm{e}}} + \int_{\Omega^e} P_i \left[\frac{\partial \widehat{\mathbf{U}}}{\partial t} - \mathbf{S} + \nabla \cdot \mathbf{F} \right] d\Omega^{\mathrm{e}} = 0$$

(Integration by Parts)

$$\boxed{- \int_{\Omega^{\mathrm{e}}} \nabla N_i \cdot \mathbf{F} \, d\Omega^e + \int_{\Gamma^{\mathrm{e}}} N_i \, [\mathbf{F} \cdot \mathbf{n}] \, d\Gamma^e}$$

Discretization

- Semi-discrete formulation:

$$\mathbf{M}\frac{\partial \hat{\mathbf{U}}}{\partial t} + \mathbf{R}(\hat{\mathbf{U}}) = \mathbf{0}$$

- Using BDF2 method:

$$\mathbf{Res}^{\mathbf{n+1}}(\hat{\mathbf{U}}^{\mathbf{n+1}}) = \frac{\mathbf{M}}{\Delta\mathrm{t}}\left(\frac{3}{2}\hat{\mathbf{U}}^{\mathbf{n+1}}\right) + \mathbf{R}(\hat{\mathbf{U}}^{\mathbf{n+1}}) - \frac{\mathbf{M}}{\Delta\mathrm{t}}\left(2\hat{\mathbf{U}}^{\mathbf{n}} - \frac{1}{2}\hat{\mathbf{U}}^{\mathbf{n-1}}\right) = 0$$

- Using Newton method:

$$[\mathbf{J}]^{\mathbf{n}}[\mathbf{\Delta U}^{\mathbf{n}}] = -\mathbf{Res}^{\mathbf{n}}$$

$$[\mathbf{J}] = \left[\frac{\partial \mathbf{Res}}{\partial \hat{\mathbf{U}}}\right]$$

- GMRES method with ILU(k) preconditioning.

Constraint Approximation

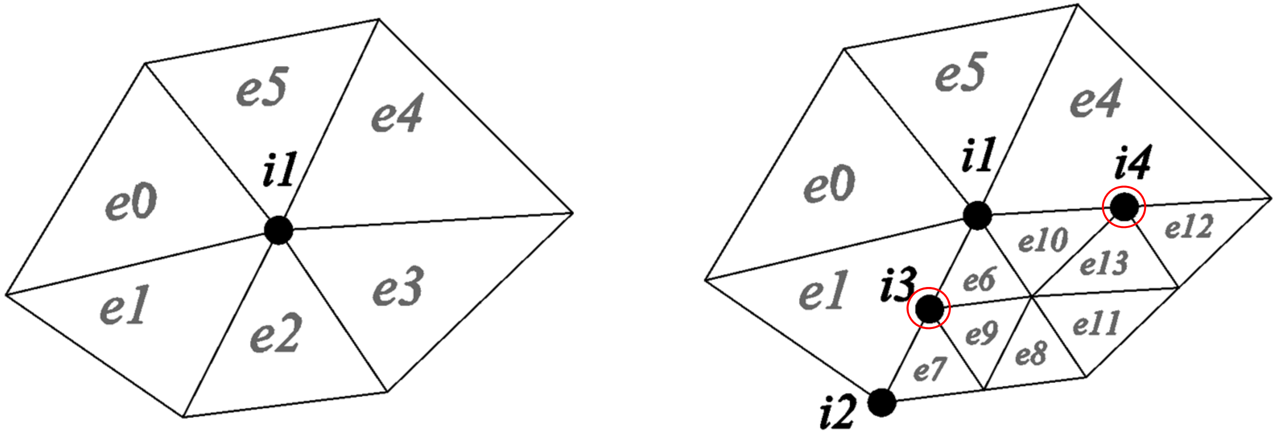

$$\mathbf{U}_{cn} = \sum_{k=1}^{nsup} \mathrm{c}_{cn_k} \mathbf{U}_{cn_k}$$

$$[\mathbf{J}]^{\mathbf{n}} [\mathbf{\Delta U}^{\mathbf{n}}] = -\mathbf{Res}^{\mathbf{n}}$$

$$\boxed{\int_{\Gamma^e} N_i [\mathbf{F} \cdot \mathbf{n}] \, d\Gamma^e}$$

Constraint Approximation

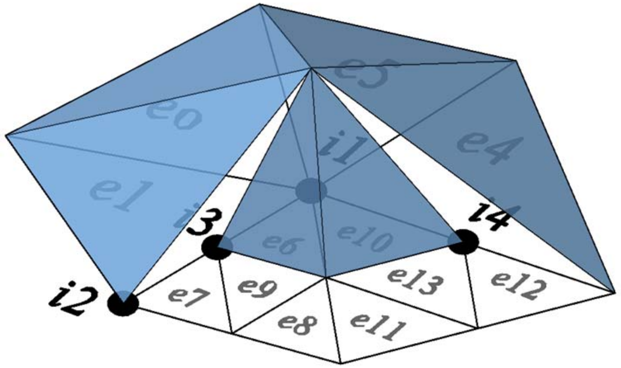

N_{i1} (after h-refinement)

$$\boxed{\int_{\Gamma^e} \underset{\uparrow}{N_i} [\mathbf{F} \cdot \mathbf{n}] \, d\Gamma^e}$$

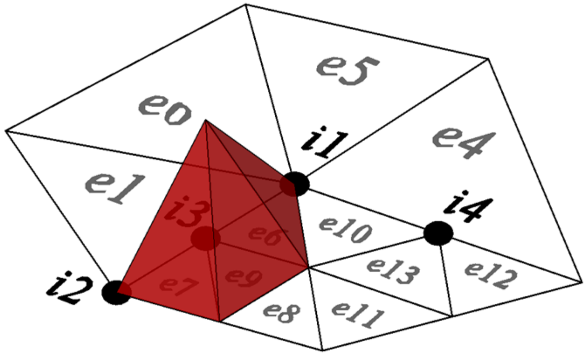

N_{i3}

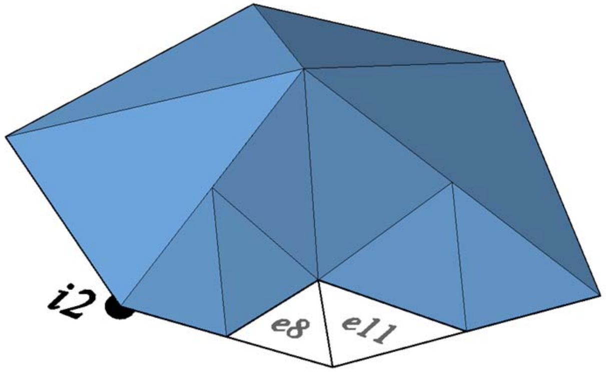

$$\widetilde{N}_{i1} = N_{i1} + \frac{1}{2} N_{i3} + \frac{1}{2} N_{i4}$$

Constraint Approximation

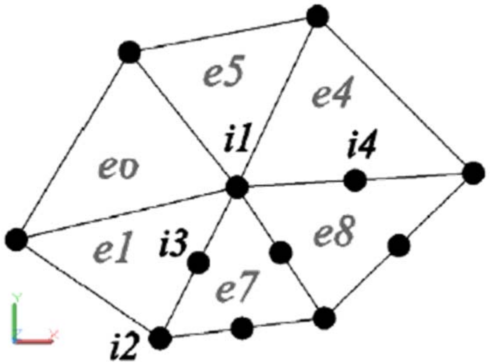

(a) 1 level of p-refinement

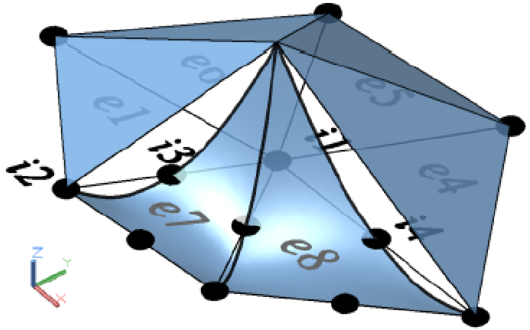

(b) N_{i1} (after p-refinement)

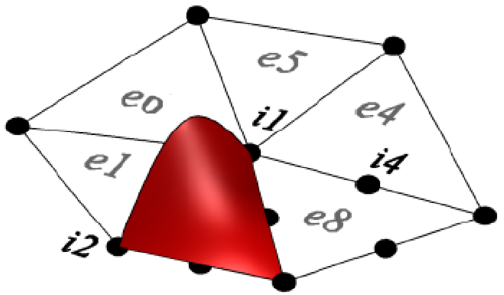

(c) N_{i3}

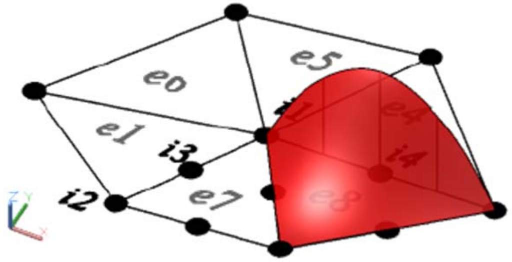

(d) N_{i4}

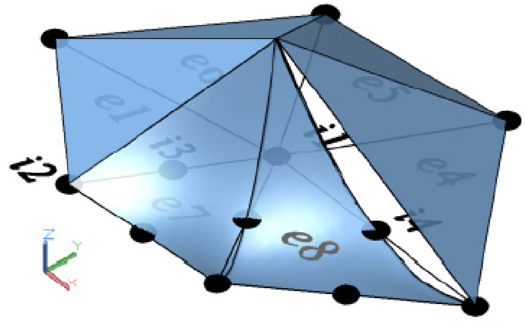

(e) $N_{i1} + \frac{1}{2}N_{i3}$

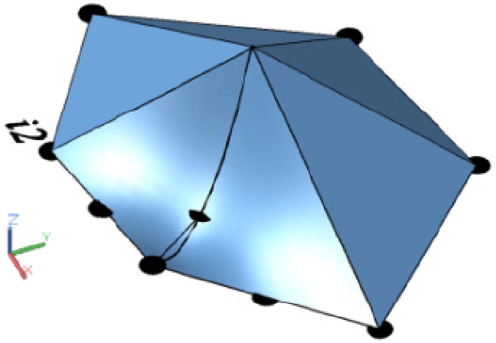

(f) $N_{i1} + \frac{1}{2}N_{i3} + \frac{1}{2}N_{i4}$

Constraint Approximation

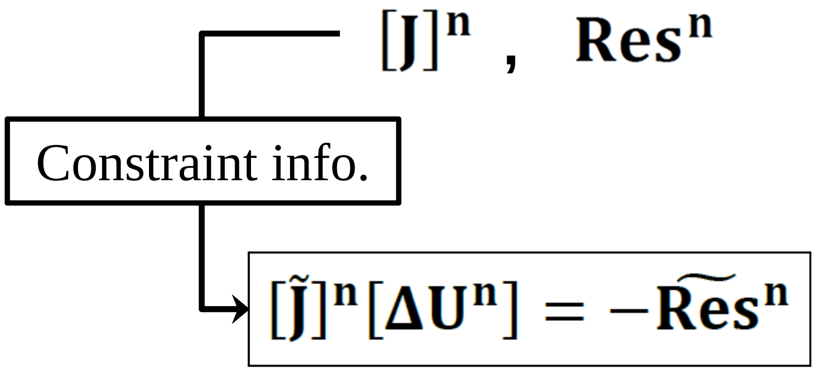

$[\mathbf{J}]^{\mathbf{n}}$, $\mathbf{Res}^{\mathbf{n}}$

Constraint info.

$$\boxed{[\tilde{\mathbf{J}}]^{\mathbf{n}}[\mathbf{\Delta U}^{\mathbf{n}}] = -\widetilde{\mathbf{Res}}^{\mathbf{n}}}$$

$$\int_{\Omega}(\widetilde{N}_i + P_i)\left[\frac{\partial\widehat{\mathbf{U}}}{\partial t} + \nabla\cdot\mathbf{F} - \mathbf{S}\right]d\Omega = 0$$

$$\widetilde{\mathbf{Res}}_{\mathbf{i}} = \mathbf{Res}_{\mathbf{i}} + \sum_{k=1}^{nhang} \mathrm{c}_{k_i}\mathbf{Res}_{\mathbf{k}}$$

Outline

- Motivation
- Mesh Modification Mechanisms
- Governing Equations and Discretization
- ➡ Adaptation Criteria
- Numerical Results
- Conclusions

Adaptation Criteria

Feature-Based Methods

- Aim to capture regions with distinguishing flow features.
- Usually use the gradients of the flow variables.
- Considered as error indicators.

- Pros
  - ➢ Simplicity.
  - ➢ Cost efficiency

- Cons
  - ➢ Ad-hoc nature. May converge to the incorrect solution.

  - Still used particularly for ***transient problems***.

Adaptation Criteria

Adjoint-Based Methods

- Target a specific functional output *f* (usually in the integral form).
- Provide error estimations.

$$\left[\frac{\partial \mathbf{R}}{\partial \mathbf{U}}\right]^T \underbrace{\left(\frac{\partial f}{\partial \mathbf{R}}\right)}_{\boldsymbol{\lambda}} = \left(\frac{\partial f}{\partial \mathbf{U}}\right)^T \quad \boxed{local\ error \approx \boldsymbol{\lambda}^T \mathbf{R}}$$

- Pros
  - A prescribed precision is ensured.
  - The obtained sensitivity data can also be utilized for design and optimization.

- Cons
  - Costly → Feasible for ***steady-state*** flows.
  - Difficult to implement.

Adaptation Criteria

Adjoint-Based Methods

$$\boxed{local\ error \approx \boldsymbol{\lambda}^T \mathbf{R}}$$

1. **Adaptation parameter 1:**
   - Adapts the mesh to reduce flow residual

$$\varepsilon_e = \sum_{l(e)} c_{l(e)} \left| [\boldsymbol{\lambda}_h^H \mathbf{R}_h(\mathbf{U}_h^H)]_{l(e)} \right|$$

2. **Adaptation parameter 2 [Venditti and Darmofal]:**
   - Adapts the mesh to reduce both flow and adjoint residuals

$$\varepsilon_e = \sum_{l(e)} c_{l(e)} \left\{ \left| [\boldsymbol{\lambda}_h^{HO} - \boldsymbol{\lambda}_h^{LO}]_{l(e)}^T [\mathbf{R}_h(\mathbf{U}_h^{LO})]_{l(e)} \right| + \left| [\mathbf{U}_h^{HO} - \mathbf{U}_h^{LO}]_{l(e)}^T \left[\mathbf{R}_h^{\lambda}(\boldsymbol{\lambda}_h^{LO})\right]_{l(e)} \right| \right\}$$

Outline

- Motivation
- Mesh Modification Mechanisms
- Governing Equations and Discretization
- Adaptation Criteria
- ➡ Numerical Results
- Conclusions

Numerical Results

- **Steady-State Cases:**
  1. Adjoint-based h-, p-, and hp-adaptation for steady inviscid flow over a four element airfoil
  2. Adjoint-based h-adaptation for steady turbulent flow over a three element airfoil
- **Unsteady Case:**
  3. Dynamic feature-based h- and p-adaptation for laminar flow over a cylinder

Adjoint-Based Adaptation for Steady State Flow over a Four Element Airfoil

- **Flow conditions:**
  - Inviscid
  - Mach = 0.2
  - Angle of attack = 0 ^{o}
- **Initial mesh:**
  - 1251 nodes
- **Functional output:**
  - Lift coefficient

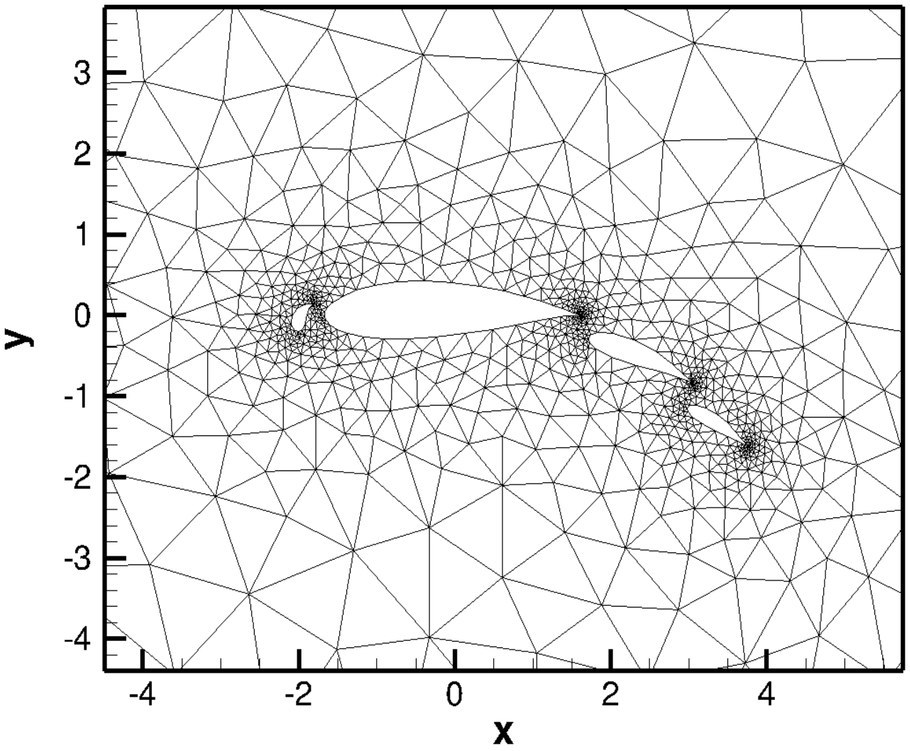

- **Purpose:**
  - Quantitative comparison of h-, p-, and hp-adaptations

Inviscid Flow over Four Element Airfoil

Case Study	Adjoint Adaptation Parameter	Adjoint Estimation
Uniform-h-refinement	-	-
H-adaptation-setting-1	1st	Low order Prolongation
H-adaptation-setting-2	1st	High order Prolongation
H-adaptation-setting-3	1st	Exact Solution
H-adaptation-setting-4	2nd	High and Low order Prolongations
P-adaptation	1st	Exact Solution
Hp-adaptation-setting-1	1st	Exact Solution
Hp-adaptation-setting-2 (h)	1st	Exact Solution

Inviscid Flow over Four Element Airfoil

Target Solution : $C_L = 5.0200$

- Asymptotic value obtained from h-adaptation on P2 elements
- Tolerance within 1.e-4

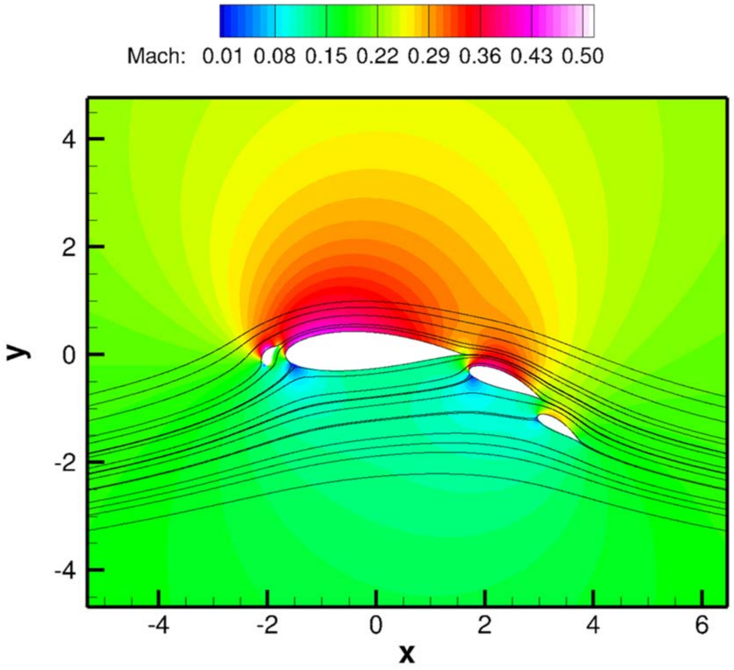

Mach number and streamlines

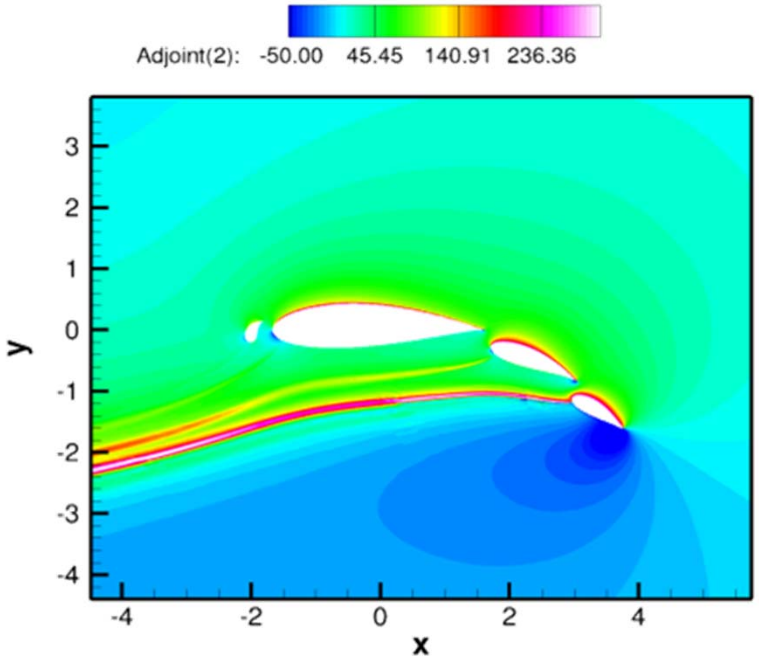

X-momentum component
of discrete adjoint

Inviscid Flow over Four Element Airfoil

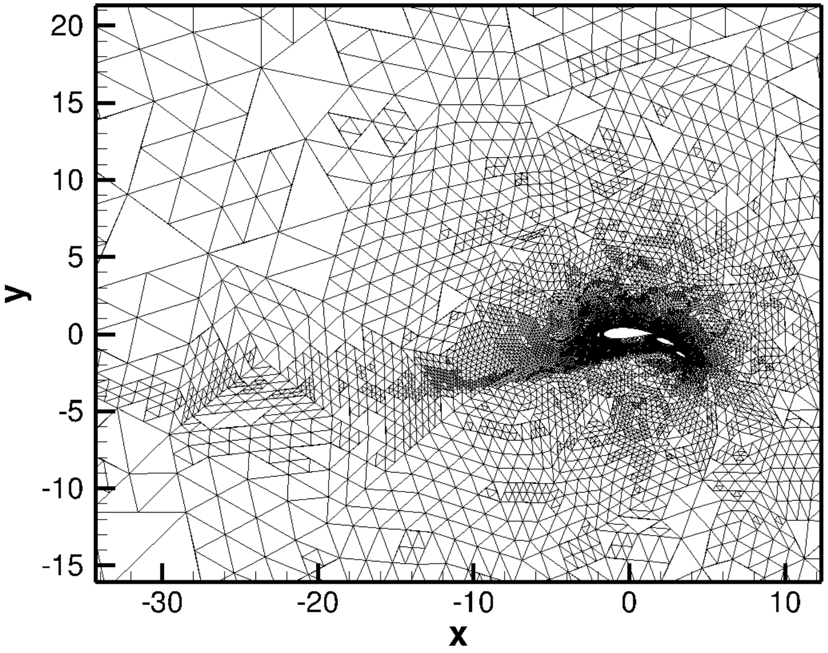

Final h-adapted mesh (setting 3)

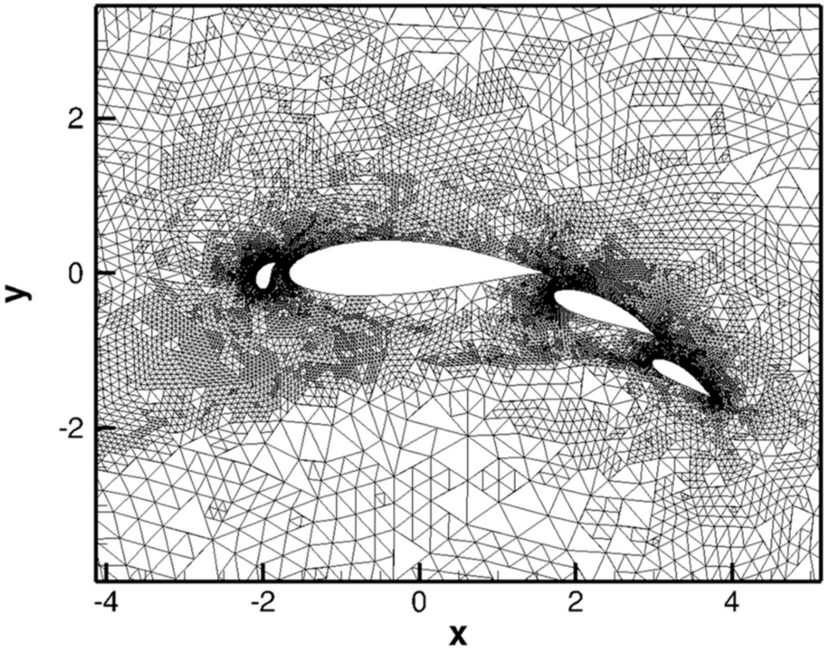

Close-up view

Inviscid Flow over Four Element Airfoil

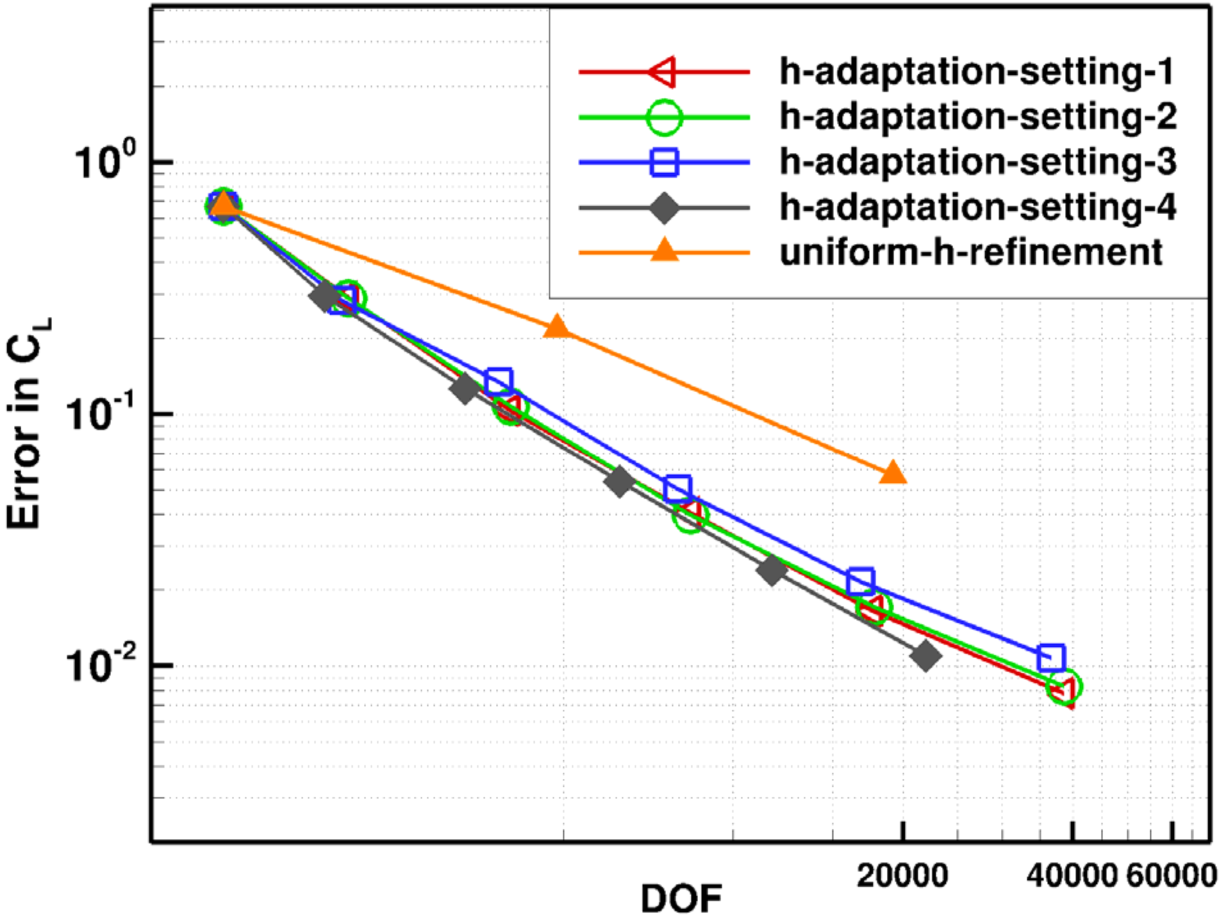

Inviscid Flow over Four Element Airfoil

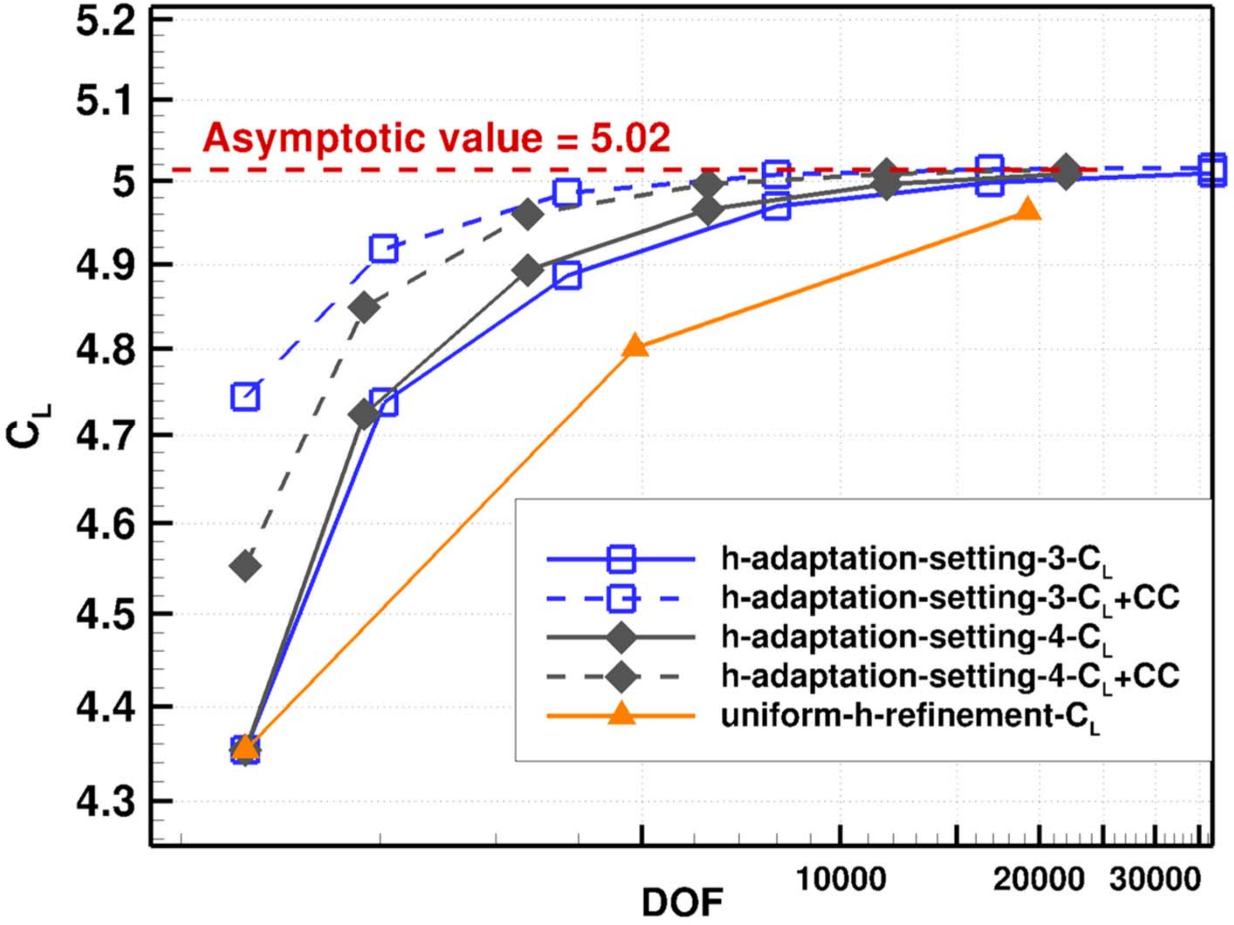

Inviscid Flow over Four Element Airfoil

P-Adaptation

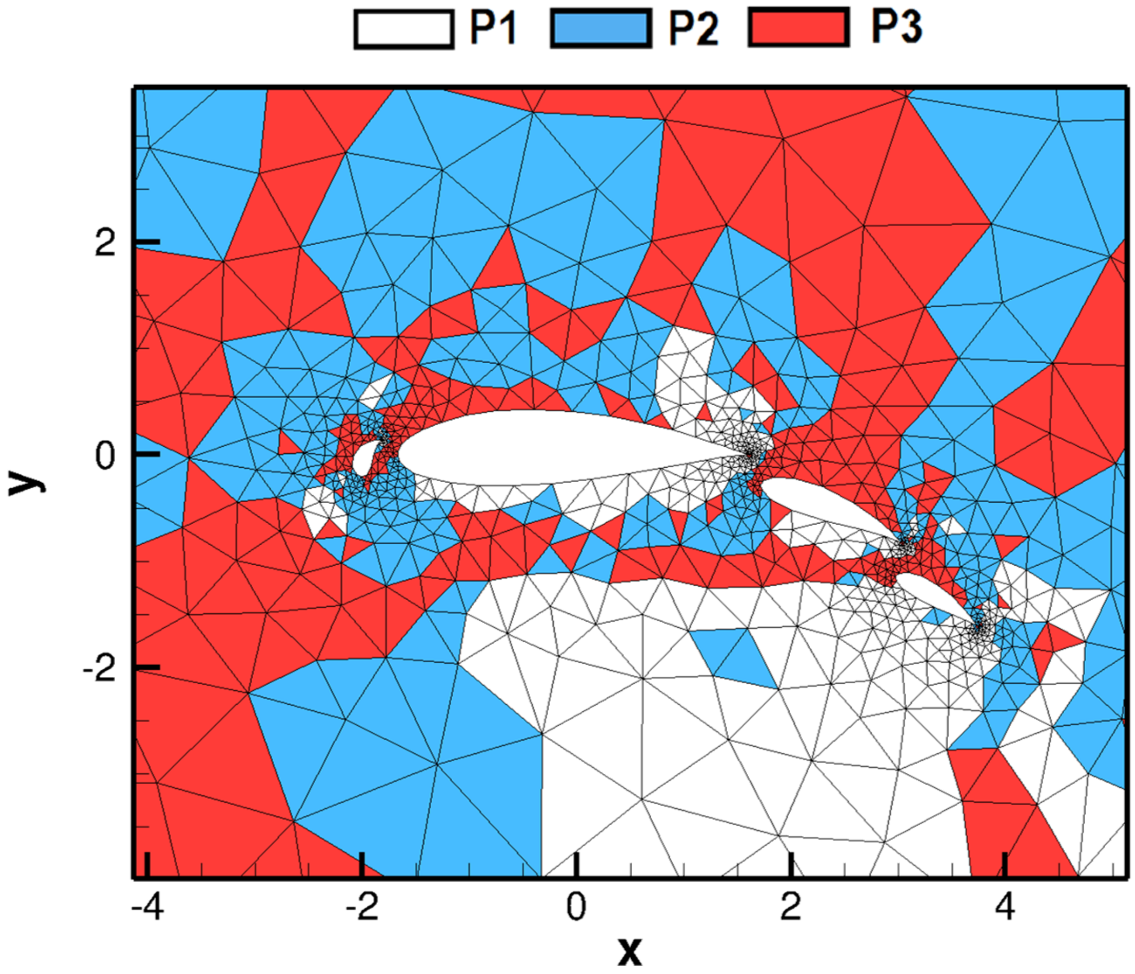

Inviscid Flow over Four Element Airfoil

Hp-Adaptation

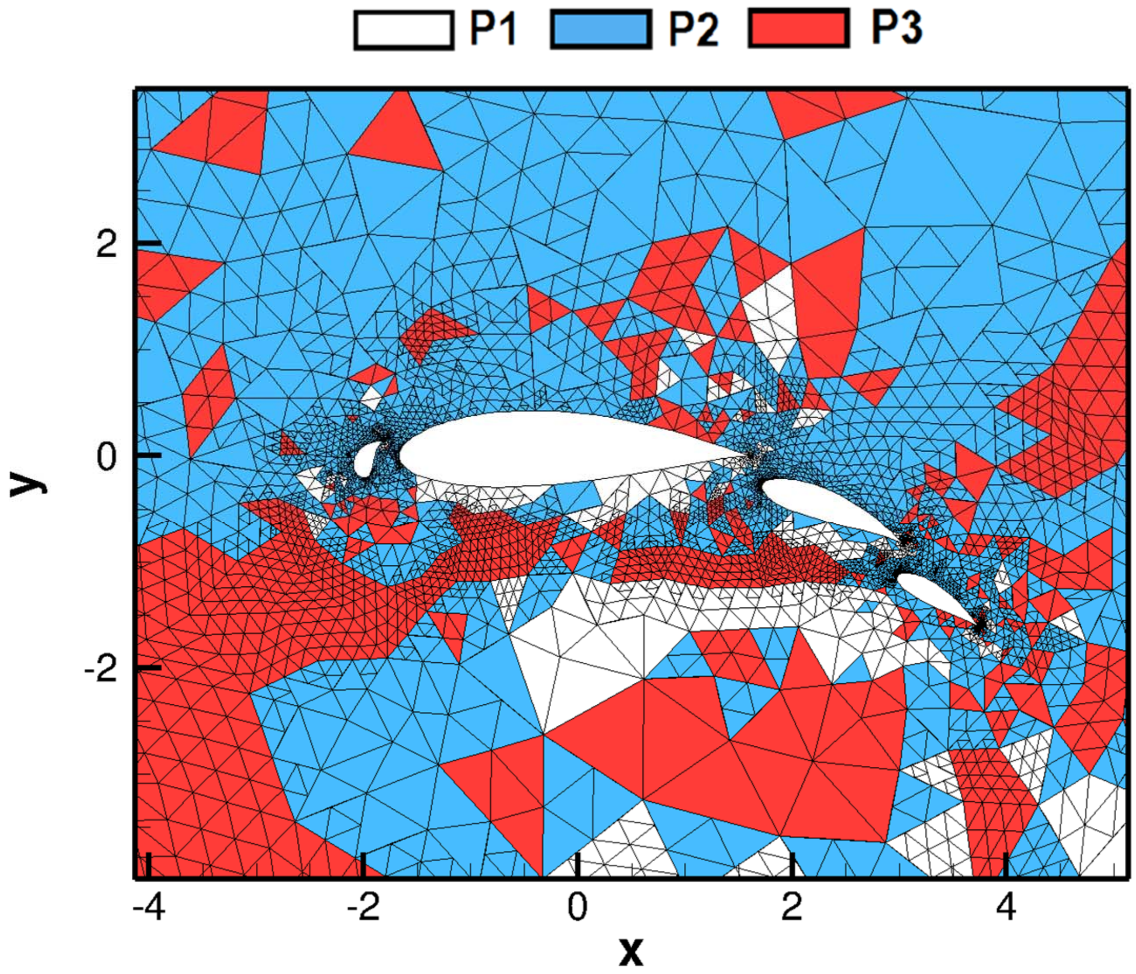

Inviscid Flow over Four Element Airfoil

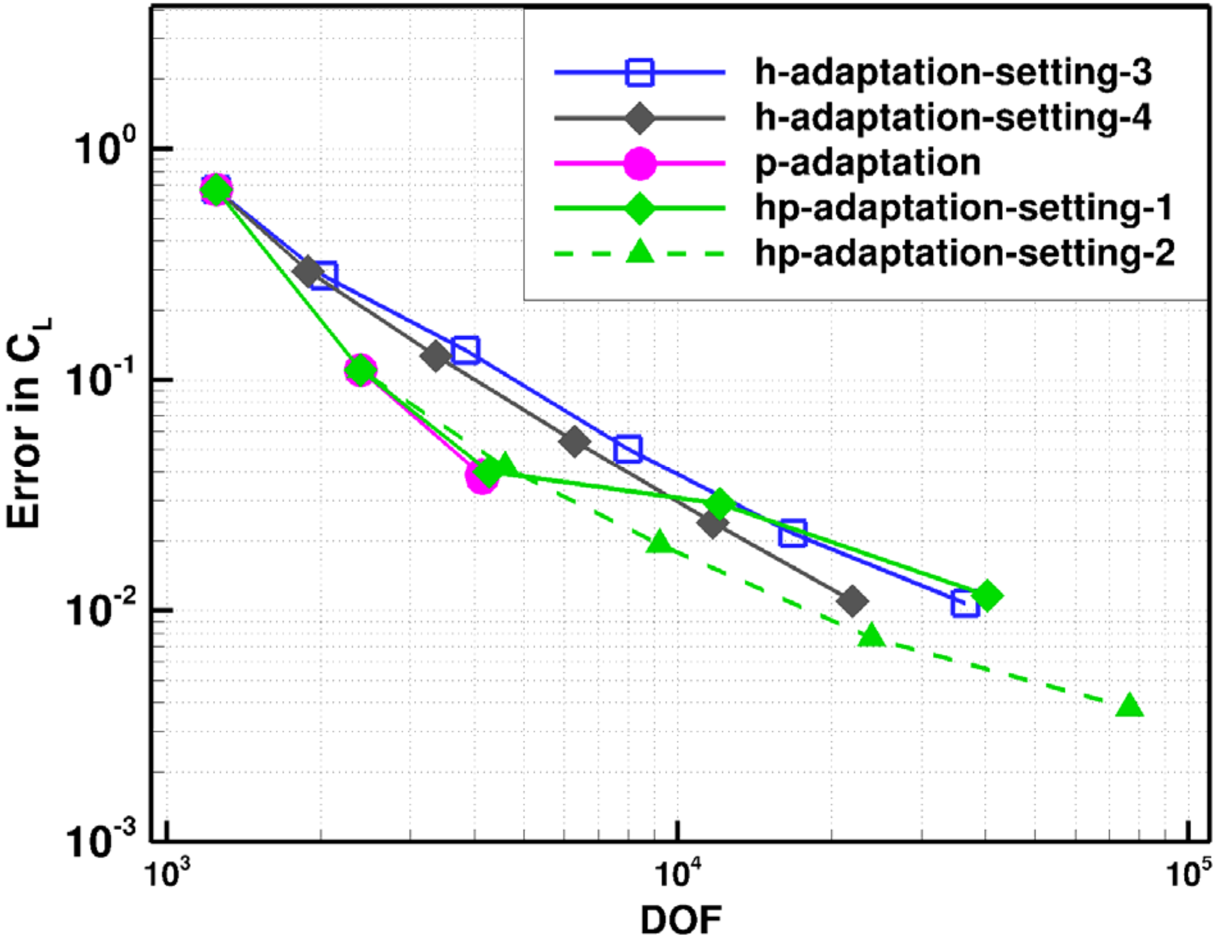

Inviscid Flow over Four Element Airfoil

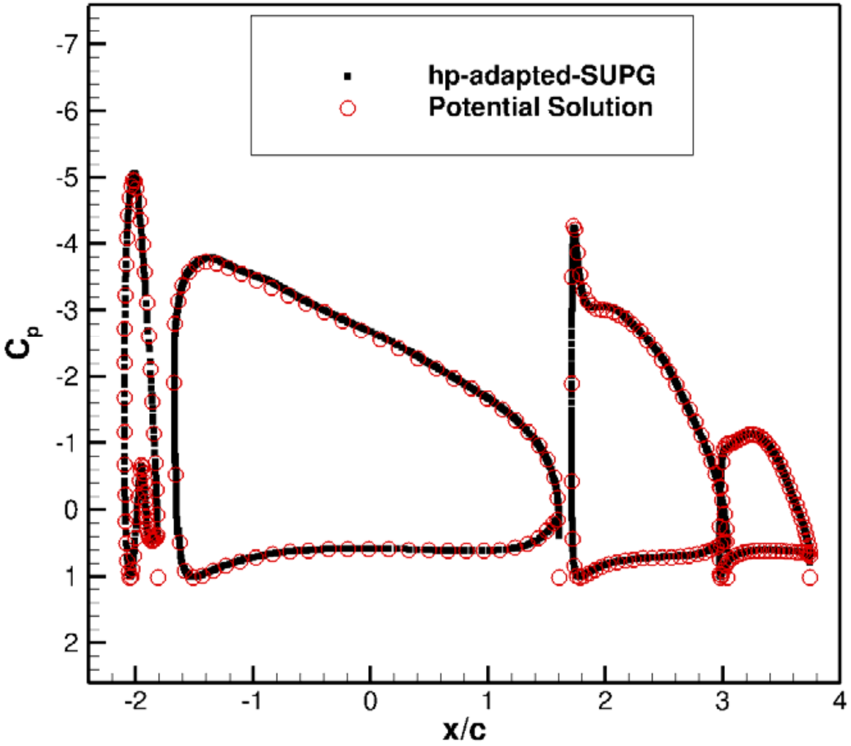

Prandtl-Glauert Correction:

$$C_{p,comp.} = C_{p,incomp.}/\sqrt{1 - M_\infty^2}$$

Adjoint-Based Adaptation for Steady State Turbulent Flow over a Three Element Airfoil

- **Flow conditions:**
  - Turbulent (Re = 9E+6)
  - Mach = 0.2
  - Angle of attack = 16.2 °
- **Initial mesh:**
  - 38973 nodes
- **Functional output:**
  - Lift coefficient

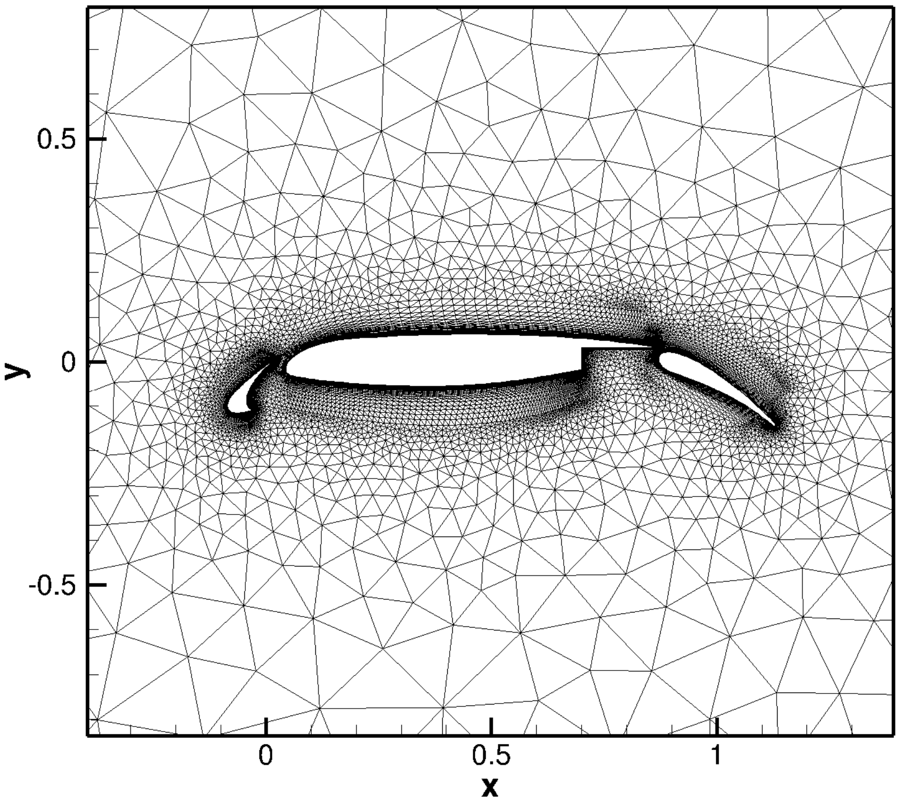

- **Purpose:**
  - Capability assessment for turbulent flows with complex geometries

Turbulent Flow over a Three Element Airfoil

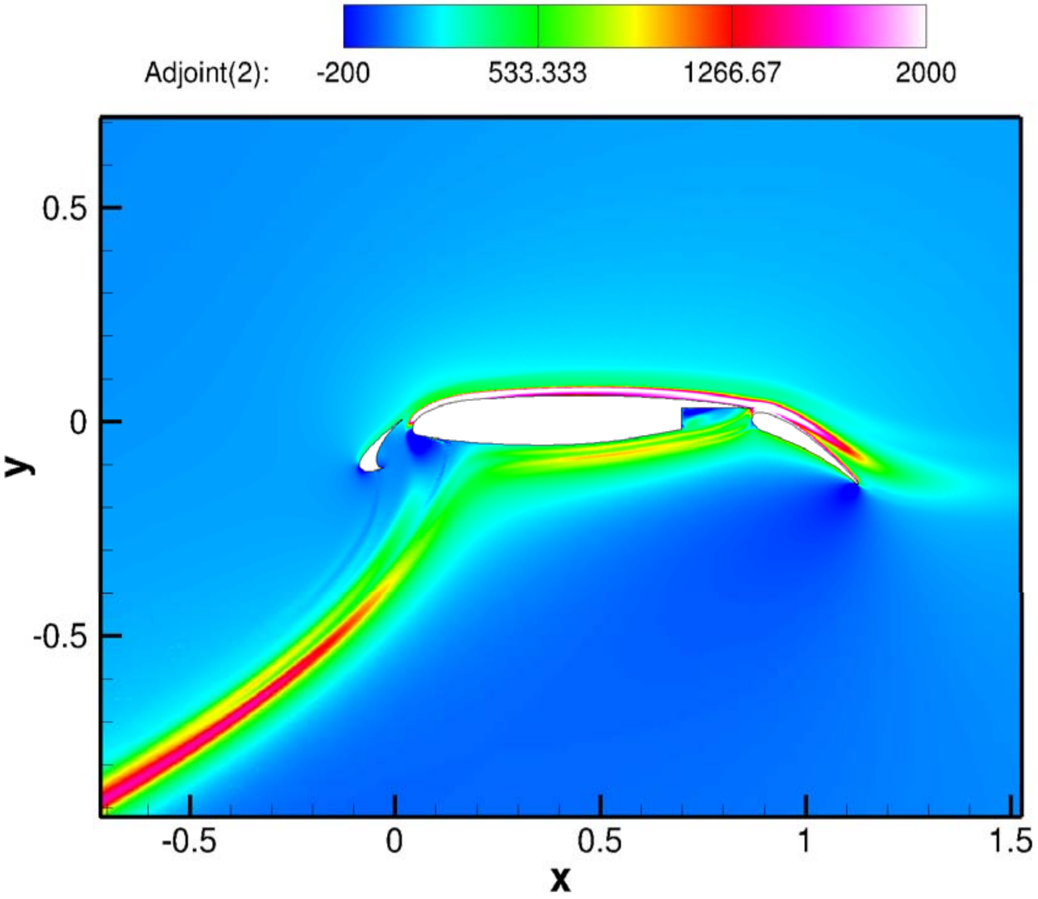

X-momentum component of discrete adjoint

Turbulent Flow over a Three Element Airfoil

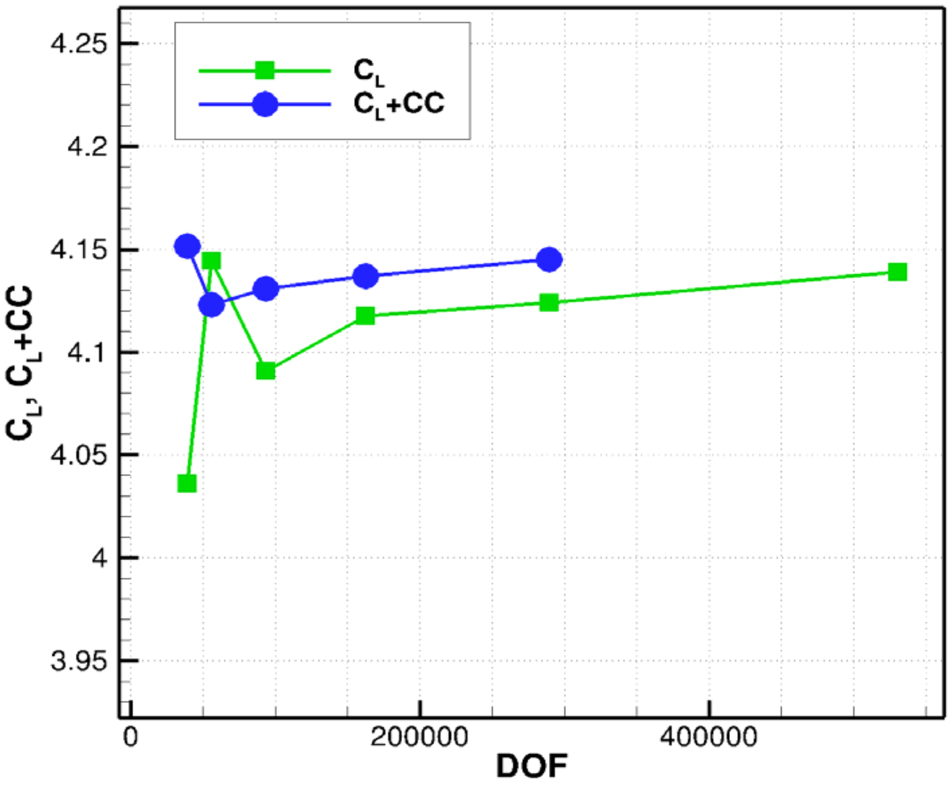

Convergence of the lift coefficient

Turbulent Flow over a Three Element Airfoil

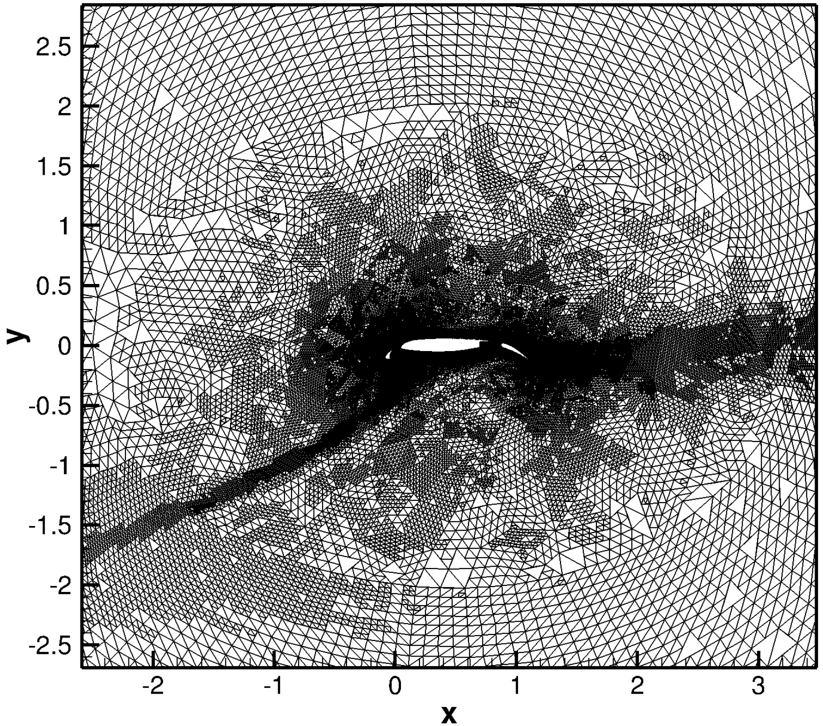

Final h-adapted mesh

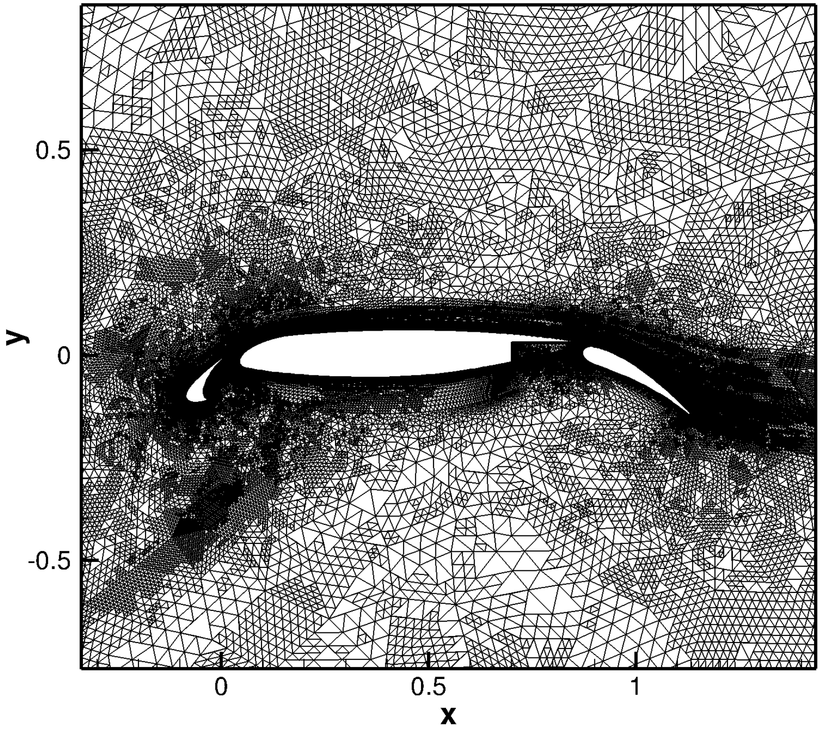

Close-up view

Turbulent Flow over a Three Element Airfoil

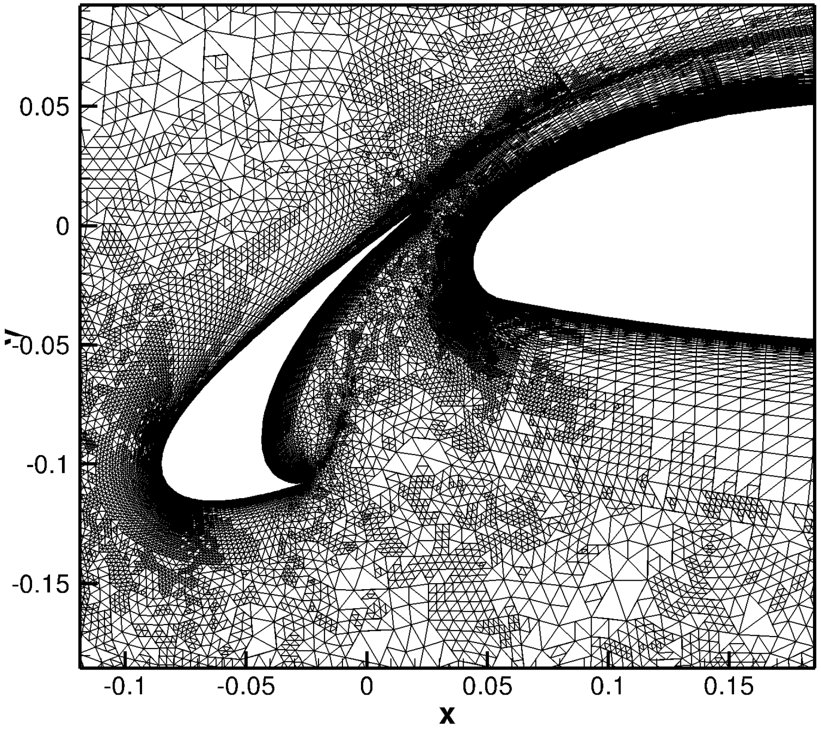

Slat and leading edge

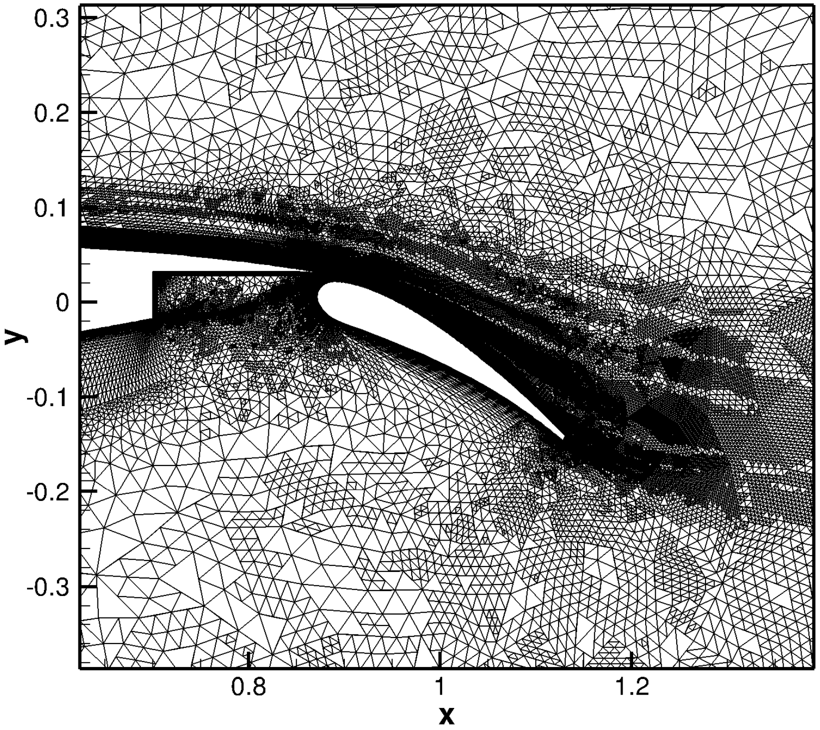

Flap cove and flap

Turbulent Flow over a Three Element Airfoil

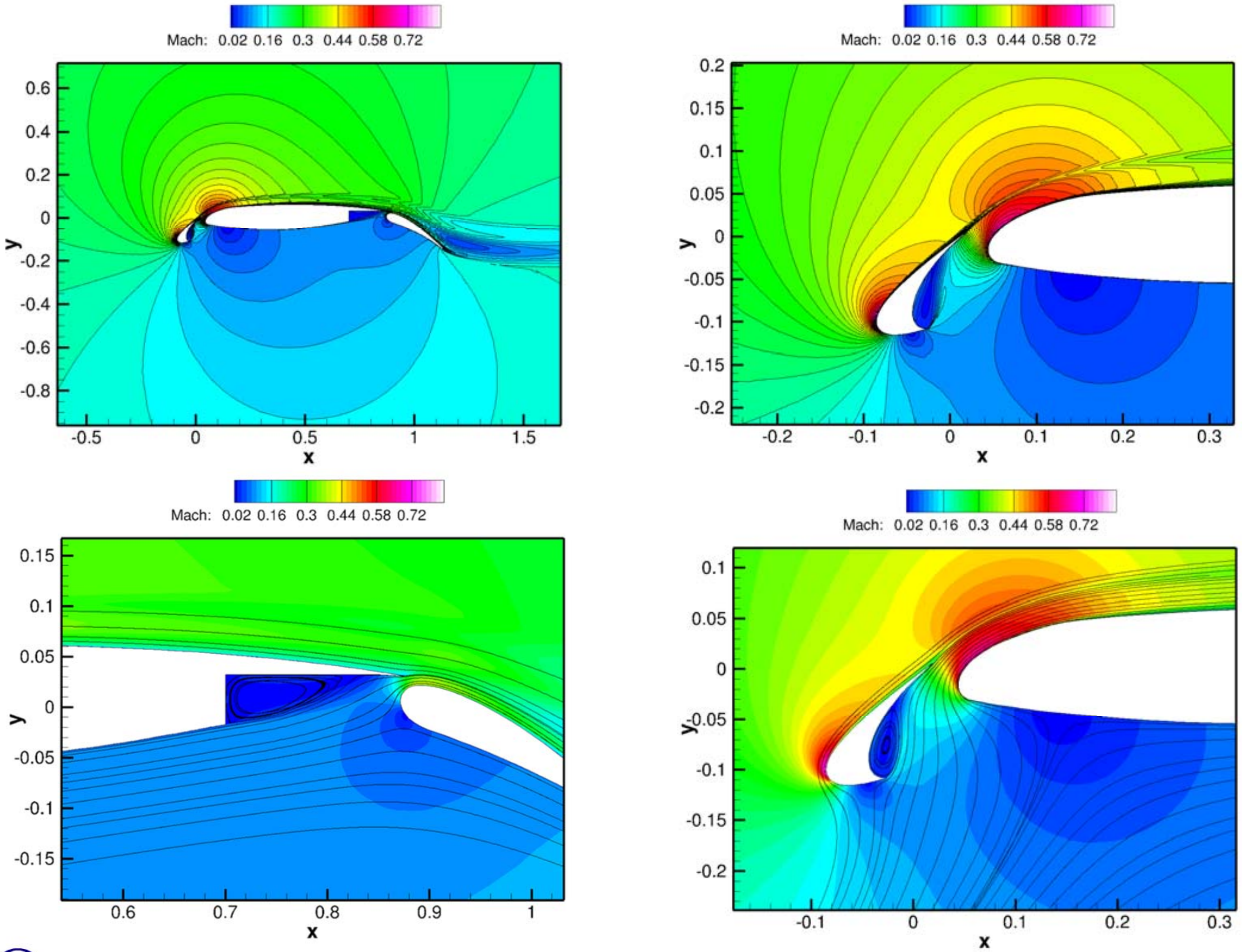

Turbulent Flow over a Three Element Airfoil

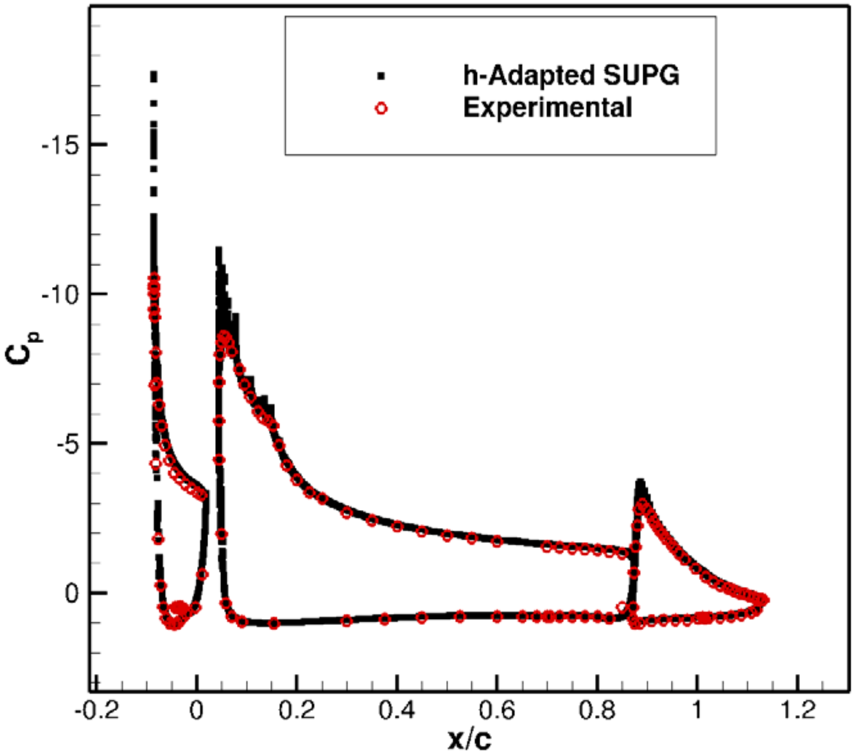

Comparison of surface pressures

Feature-Based Adaptation for Vortex Shedding Flow over a Cylinder

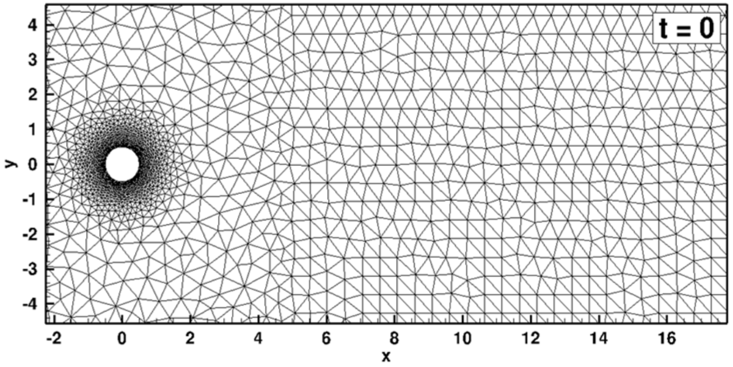

- **Flow conditions:**
  - Laminar (Re = 100)
  - Mach = 0.2
- **Adaptation parameter:**
  - Magnitude of velocity gradient
- **Purpose:** Capability assessment for dynamic adaptation
- **Studied cases:**
  - Case 1: uniform P1 elements
  - Case 2: uniform P2 elements
  - Case 3: h-adaptation on P1 elements. Max. refinement layer = 3
  - Case 4: p-adaptation using P1 to P3 elements

Dynamic Adaptation on Vortex Shedding Flow

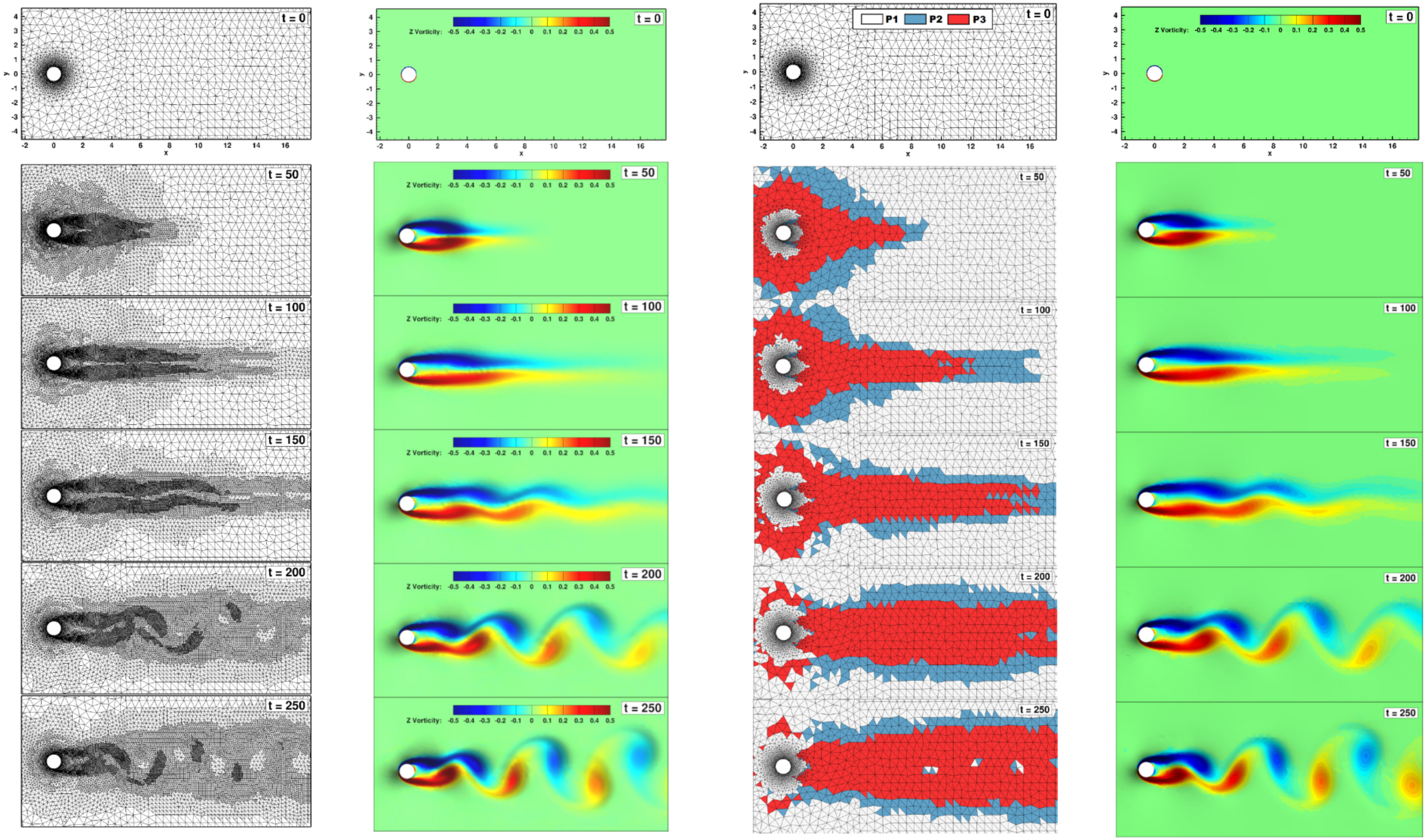

Dynamic Adaptation on Vortex Shedding Flow

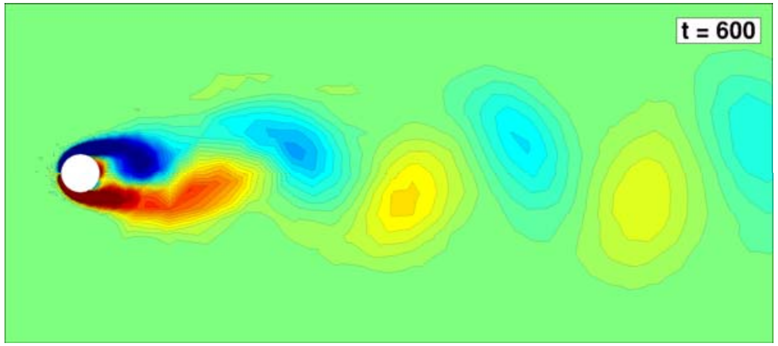

Case 1: Uniform P1 elements

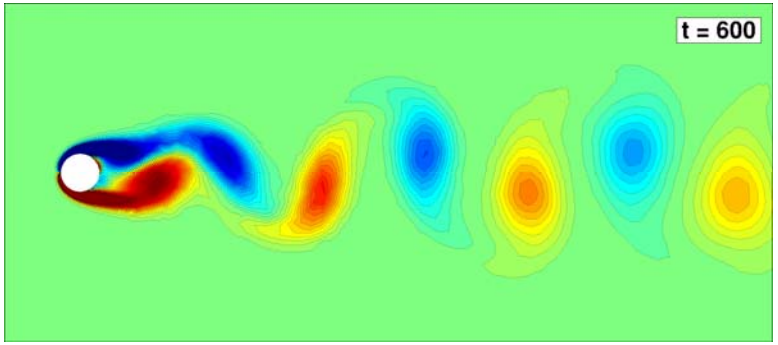

Case 2: Uniform P2 elements

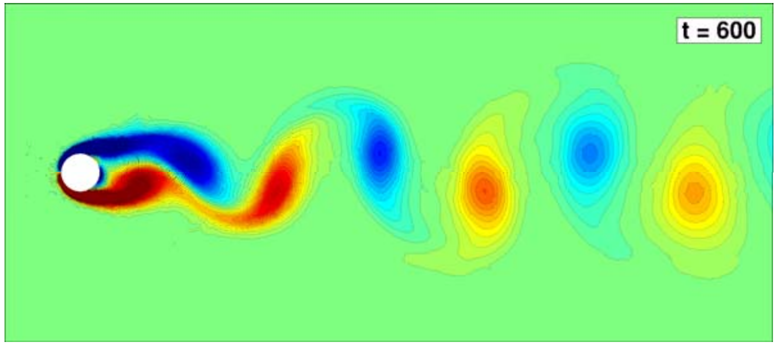

Case 3: h-adaptation on P1 elements

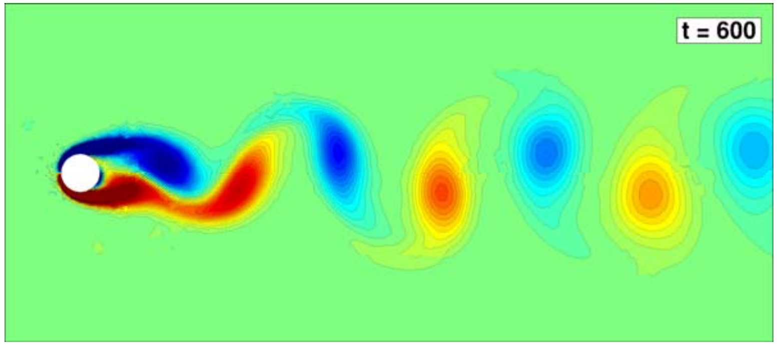

Case 4: p-adaptation using P1 to P3

Outline

- Motivation
- Mesh Modification Mechanisms
- Governing Equations and Discretization
- Adaptation Criteria
- Numerical Results
- ➡ Conclusions

Conclusions for Adaptive Meshing

- A dynamic adaptation technique has been successfully coupled with a higher order (SUPG) finite-element scheme.
- The problem of hanging nodes has been addressed by constraint approximation method.
- The advantage of the method is that it can be implanted simply by adding a condensation step to an existing SUPG or any other continuous Galerkin method.
  - ➢ Particularly important for multi-disciplinary simulations.
- Method is applicable to 3D.

Conclusions for Adaptive Meshing

- Numerical results have been shown for both steady state and unsteady problems.
- In steady-state problems, adjoint-based adaptation has been employed for both inviscid and turbulent flows.
- In unsteady problems, feature-based adaptation has been employed for a laminar flow.
- Functioning of refinements and derefinement mechanisms were verified in h- and p- and hp-adaptations.
- In all cases, the adapted solutions improved the solution’s accuracy.